NTIA Report 86-192

EHF Telecommunication System Engineering Model

Kenneth C. Allen

U.S. DEPARTMENT OF COMMERCE
Malcolm Baldrige, Secretary

Alfred C. Sikes, Assistant Secretary
for Communications and Information

April 1986

PREFACE

This report and the associated project work have been sponsored by the Propagation Engineering Branch of the United States Army Information Systems Engineering Agency (USAISEA). Their contributions and guidance are gratefully acknowledged.

The use of trade names in this report is necessary to impart relevant information and does not imply a product endorsement by the U.S. Government.

TABLE OF CONTENTS

LIST OF FIGURES

LIST OF TABLES

EHF TELECOMMUNICATION SYSTEM ENGINEERING MODEL

Kenneth C. Allen*

An EHF Telecommunication System Engineering Model (ETSEM) has been developed as an aid in the design of line-of-sight (LOS) communciation systems from 10 to 100 GHz. ETSEM provides tabulation of path geometry parameters and analyzes ray-path and Fresnel zone clearances to help the engineer design the path. ETSEM also predicts the performance (availability) of both digital and analog systems based on state-of-the-art EHF propagation models and equipment specifications. Attenuation by rain, clear-air absorption, and multipath are modeled. These are expected to essentially determine the statistics of link availability as limited by propagation impairments. Performance may be predicted for any interval of months of the year. A climatological data base for North America and Europe provides parameters for the propagation models. ETSEM has been implemented on a desk-top computer. Weaknesses and limitations of the model are discussed and improvements are suggested.

Key words: clear-air absorption; line of sight; millimeter wave; multipath fading; propagation; rain attenuation; system performance; telecommunications

1. INTRODUCTION

This report describes the EHF Telecommunication System Engineering Model (ETSEM). ETSEM was developed for the U.S. Army Information Systems Engineering Agency (USAISEA) to aid in the engineering design of line-of-sight (LOS) communication systems utilizing the radio spectrum from 10 to 100 GHz.

The model predicts the performance (availability) of communication systems based on models of Extremely High Frequency (EHF) radio propagation and equipment specifications and provides other information useful for the design of such systems. The engineer is able to vary design parameters and see immediately the resulting change in the predicted performance of the system. This allows the engineer to efficiently examine tradeoffs to find economical designs that meet the communication requirements.

The model predicts the performance of both analog and digital communication systems. Performance is measured for digital systems by the bit error rate (BER) and for analog systems (FM/FDM) by the signal-to-noise ratio (S/N) in the worst channel. Performance may be predicted for any interval of months of the year. The ability to predict performance for periods as short as one month is important if accurate predictions of performance are to be made for short-term tactical installation.

---

*The author is with the Institute for Telecommunication Sciences, National Telecommunications and Information Administration, U.S. Department of Commerce, 325 Broadway, Boulder, Colorado 80303.

The model has been implemented on an HP9825 desk-top computer. The computer code is divided into modules for different tasks. These modules can be separated into three basic groups.

The first group of modules serves as an aid in the selection and design of the propagation path. Antenna heights and Fresnel-zone clearances as well as antenna azimuths and elevation angles are computed. These modules of the computer program are similar to the corresponding modules of ADSEM, a computer model for lower frequencies developed earlier by Hause and Wortendyke (1979) at the Institute for Telecommunication Scienes (ITS).

The second group of modules combines the link equipment gain with the predicted cumulative distribution of propagation losses to produce a predicted cumulative distribution of the received signal level (RSL) from which the system performance can be determined.

The third group of modules is composed of models that predict the system performance based on the cumulative distribution of the RSL.

The models in each group of modules are discussed in more detail in sections 2, 3, and 4 of this report.

A climatological data base for North America and Europe is included in ETSEM. The parameters needed for the various propagation models are interpolated from this data base using the geographic coordinates of the midpoint of the path under study. This greatly reduces the amount of data entry required when analyzing a communication system. If desired, the climatological data may be manually entered.

Section 6 of this report contains recommendations for improvement and verification of ETSEM as well as suggestions of further experimental and model development work that is needed for EHF systems.

2. SYSTEM INSTALLATION MODELS

2.1 Earth Geometry Module

The purpose of the Earth Geometry Module is to provide tabulation of the following data:

- tower (or potential tower) designation,
- tower base elevations above mean sea level,
- tower location (latitude and longitude),
- the great circle distance between towers,
- azimuth from true north at each tower to the other tower,
- magnetic azimuths at each tower to the other tower,
- map crossing, i.e. the latitude and longitude of the points where the path crosses specified map boundaries,

- distances from map crossings to the towers.

2.1.1 Earth Geometry

The model used to compute earth geometry is unavoidably inexact but should be very satisfactory for engineering line-of-sight paths. The Earth Geometry Module defaults to the International Spheroid for these calculations but provision is made for the selection of other spheroids.

Spheriods in use today include the Clark Spheroid of 1866, the Malayan Spheroid, the Bessel Spheroid, the Australian National Spheroid, and the International Spheroid. Table 2-1 lists the equatorial and polar radii in kilometers.

Table 2-1. Earth Radii for Various Spheroids

Spheroid	Equatorial Radius (km)	Polar Radius (km)
Internationl	6378.388	6356.912
Clark 1866	6378.2064	6356.5838
Clark 1880	6378.249145	6356.514869
Everest	6377.276345	6356.075415
Bessel	6377.397155	6356.078963
Australian National	6378.160	6356.7745
Airy	6377.563396	6356.256910
Fischer	6378.155	6356.77332
Maylayan	6377.304063	6356.103039

The semi-major and -minor axes (in kilometers) of the different spheroids are contained in ETSEM. A map showing which areas of the world are based on the various spheroids is contained in U.S. Department of the Army (1967). Thus, for greater accuracy, the applicable spheroid constants can be used in any particular area of the world. The spheroid used in preparing the maps from which the profile values are taken should be selected.

However, lest sight is lost of the relative importance of the accuracy required of the spheroid constants, it should be pointed out that the difference in path length and therefore in transmission loss in dB using the widest spread of values in Table 2-1 is less than one percent. The difference in free space loss is less than 0.03 dB.

The model used for the computations is the one proposed by Thomas (1970). The initial point latitude, A, and longitude, B, as well as the terminal point latitude, X, and longitude, Y, are entered. The great circle path length (km), S; azimuth from the initial point, u; and azimuth from the terminal point, v, are computed. The program assumes positive values are north or east and negative values are south or west. The azimuth values are given in degrees east of north. An example of the output tabulation is presented in Table 2-2.

2.1.2 Map crossings

Map crossings are given as the latitude and longitude of the points where the path crosses the boundaries of maps as specified by the user. They are computed to aid in determining the terrain profile along the path from topological maps. The latitude or longitude of a map boundary is entered and the longitude or latitude, respectively, of the point where the path crosses the map boundary is computed. This enables the drawing of the path on individual tropographic maps for the scaling of the path profile.

Map crossings are computed by successive approximations in which values of forward azimuth to the map crossing point are compared with the path forward azimuth to provide error values to measure convergence. If values of latitude, E, or longitude, F, of the map boundary are given, then F or E, respectively, are calculated as follows:

1. Using the algorithm by Thomas (1970), the azimuth, u, from (A,B) along the great circle path to (X,Y) is calculated.
2. The first estimate of E or F is calculated by linear interpolation using
$$E = A + (X-A)(F-B)/(Y-B)$$
or
$$F = B + (Y-B)(E-A)/(X-A).$$
3. Using the Thomas algorithm, the azimuth, w, from (A,B) to (E,F) is calculated.
4. The azimuth error, e, is then calculated as
$$e = w - u.$$
5. The next estimate of E or F is now calculated using
$$E = E - ke$$
where $k = \pi(F-B)/(180\cos(B)\cos^2(u))$
or
$$F = F - ke$$
where $k = \pi(E-A)\cos(B)/180\sin^2(u)$.
6. The azimuth, w, is calculated.
7. The azimuth error, e, is calculated.
8. If the last error is greater than the previous one, the sign of k is changed and the steps are repeated beginning at step 5. If the last error is less than the previous one, then stop if the magnitude of the error is less than 0.01 seconds. Otherwise, continue at step 5.

Table 2-2. Example Output of the Earth Geometry Module

Earth Geometry
Lee Hill to Receiver Path

Left Site

Site Name		Lee Hill
Site Designator		LEE
Tower Number		1
Elevation Above Mean Sea Level	(meters)	2283.6
Latitude	(Degrees)	40 04' 00.0"N
Longitude	(Degrees)	105 22' 00.0"W
Declination from TRUE North	(Degrees)	00' 00.0"E
Azimuth from TRUE North to RCV	(Degrees)	115 15' 26.8"
Azimuth from MAGNETIC North	(Degrees)	115 15' 26.8"

Right Site

Site Name		Receiver
Site Designator		RCV
Tower Number		1
Elevation Above Mean Sea Level	(meters)	1611.9
Latitude	(Degrees)	40 00' 00.0"N
Longitude	(Degrees)	105 11' 00.0"W
Declination from TRUE North	(Degrees)	00' 00.0"E
Azimuth from TRUE North to LEE	(Degrees)	295 22' 31.3"
Azimuth from MAGNETIC North	(Degrees)	295 22' 31.3"

Great Circle Distance Between Towers(D)	(km)	17.311
Earth Spheroid Name		International
Equatorial Radius	(km)	6378.3880000
Polar Radius	(km)	6356.9120000

An example of the output tabulation of the map crossings is presented in Table 2-3.

2.2 Path Profile and Ray-Path Module

The purpose of this module is to help provide the designer with accurate information about the radio path. The goals are optimum selection of antenna heights and the preparation of foundation information to estimate the radio path reliability.

Several simple models are used to find parameters that are required in various steps of the system design. These models are needed to calculate ray path geometry, Fresnel zone clearance, minimum atmospheric layer penetration angle, mean atmospheric pressure along the ray path, and mean height of the ray path above ground.

In modeling ray paths, the earth and atmosphere are often idealized to a spherical system. A spherical earth is assumed and terrain heights are often given with respect to sea level. The atmosphere is treated as having a spherical structure concentric with the earth so that atmospheric parameters are a function of height only. It is convenient to further idealize our concepts and model the refractivity as proportional to height. Under these conditions a ray path follows the arc of a circle. If the geometry is then distorted so that the ray path becomes a straight line, the earth remains spherical but with a different radius. Thus we may conveniently imagine ray paths as straight lines so long as we are willing to imagine these ray paths over an earth with an "effective radius". The effective radius of the earth is found by multiplying the true radius by a constant called the k factor. The factor k is dependent on the proportionality factor of refractivity with height. The k factor is a common way of describing atmospheric conditions and has a typical value of about 4/3.

The geometry of the ray path is considered in section 4.2.15 of MIL-HDBK-416 (Department of Defense, 1977a) and the expression for the height of the ray path, h, in meters above mean sea level (msl) is computed as follows:

$$h = d^2/12.75k + d[(h_2 - h_1)/D - D/12.75k] + h_1 \qquad (2\text{-}1)$$

where h_1 = the antenna height in meters above msl where d = 0,
h_2 = the antenna height in meters above msl where d = D,
d = the distance along the path in km,
D = the length of the path in km,
k = the Earth's radius factor.

Because the ray path depends on the k factor, some clearance over obstacles along the path should be included in the design of the path. This clearance is

Table 2-3. Example of Map Crossing Output of the Earth Geometry Module

Intermediate Coordinates (Map crossings)
Lee Hill to Receiver Path

Latitude deg min sec	Longitude deg min sec	Distance (km) from: Lee Hill	Receiver
40 03' 16.5"N	105 20' 00.0"W	3.15	14.17

usually measured in Fresnel zones. In MIL-HDBK-416 (Department of Defense, 1977a), section 4.2.18, an equation is provided for calculating the nth Fresnel-zone radius, R_n, on a plane perpendicular to the path:

$$R_n = 17.3\left(\frac{n}{f}\right)^{1/2}\left(\frac{dD}{D} - d^2\right)^{1/2} \quad m, \qquad (2\text{-}2)$$

where f = frequency in GHz. The clearance, C, is the distance between the top of the obstacle directly beneath the ray path and the ray path in meters.

The number of Fresnel zones, n, that this clearance is equal to, is given by the following expression:

$$n = \frac{3.34fDC^2}{dD - d^2} \times 10^{-3} \qquad (2\text{-}3)$$

For all entered values of d along the path, the clearance is calculated in units of the number of first Fresnel zones, i.e. C/R_1, and the minimum value along with the corresponding value of d is noted.

Under some conditions layers form in the atmosphere and the resulting changes in refractivity with height can cause significant changes in ray paths. The direction of rays are more easily affected the shallower their angle of penetration through the layers. Some indication of how susceptable an installation may be to the effect of layers is given by computing the minimum angle of penetration with respect to a spherical atmosphere assuming some k factor, say 4/3.

The take off angle, β, is the angle between the horizontal plane and the tangent to the ray path in the great circle plane at an antenna. When d = 0,

$$\beta_1 = \tan^{-1}\frac{h_2 - h_1}{1000 \times D} - \frac{D}{12750k} \qquad (2\text{-}4)$$

when d = D,

$$\beta_2 = -\tan^{-1}\frac{D}{12750k} + \frac{h_2 - h_1}{1000 \times D} \qquad (2\text{-}5)$$

If $\beta_1 < 0$ and $\beta_2 < 0$, i.e. the arrival angles at both ends of the path are below horizontal, then the minimum angle of penetration will be 0 at some point along the path. If $|\beta_1| < |\beta_2|$, the minimum angle of penetration is $|\beta_1|$ for $k > 0$. If $|\beta_1| > |\beta_2|$, the minimum angle of penetration is $|\beta_2|$ for $k > 0$.

Atmospheric pressure is an important parameter in the computation of clear air absorption which is discussed in section 3.3. To calculate the mean atmospheric

pressure along the path, the expression for pressure, p, as a function of altitude, h, in meters above mean sea level provided in List (1951), p. 266, is used:

$$p = 101.3(1 - 2.26h \times 10^{-5})^{5.2553}, \qquad (2\text{-}6)$$

where p is in kilopascals (kPa). One kilopascal equals 10 millibars. The mean pressure along the ray path is calculated by averaging 10 values calculated for equidistant points along the path for k = 4/3.

An example of one of the tabular outputs of this module is given in Table 2-4. For the various k factors input, the relevant path clearance values are calculated and printed.

Another tabular output is given in Table 2-5. Here the antenna heights necessary to meet specified minimum path clearance requirements for a selected k factor are given.

A third tabular output available is a summary of the path profile. An example is given in Table 2-6.

An example of the graphical output available is shown in Figure 2-1. The path terrain profile is drawn and ray paths (and Fresnel zones) for entered k factors are plotted.

3. PROPAGATION MODELS

3.1 Introduction

There are many propagation effects that may degrade the performance of LOS-EHF telecommunication systems. Fortunately, it is not necessary to model all of them in order to be able to predict the availability of the communication link. Only the propagation effects that essentially determine the cumulative distribution of the transmission loss need to be considered. In addition, since it is usually desired that the system be available more than 90 percent of the time, only the propagation effects that contribute to the greater levels of attenuation that are exceeded smaller percentages of the year need to be included. Thus, for example, although scintillation, which normally subsides during rain, often attenuates the signal by several decibels (dB), it does not contribute to the level of attenuation exceeded less than a few percent of the year, normally caused by rain, and therefore does not need to be included in order to predict availability.

All propagation models used predict cumulative distributions of the attenuation caused by individual propagation effects. The combination of these distributions into a total cumulative distribution of transmission loss for small percentages of the year is discussed in section 3.5.

Table 2-4. Example of Path Clearance Output of the Terrain Profile and Ray Path Module

Terrain Profile and Ray Path Information
Lee Hill to Receiver Path

COORDINATES:

Site	Latitude	Longitude	Elevation Above MSL	Antenna Ht. Above Grnd
LEE :	40 04' 00.0"N	105 22' 00.0"W	2283.6m	80.0m
RCV :	40 00' 00.0"N	105 11' 00.0"W	1611.9m	60.0m

Path Length is 17.31 kilometers

RAY PATH MINIMUM CLEARANCE:

For an Earth Radius Factor of k= 1.33:

Absolute clearance is 55.95 meters at 17.31 km from LEE.
Minimum clearance is 20.46 times the first Fresnel Zone
Radius at 42.00 GHz, and 15.00 km from LEE.

For an Earth Radius Factor of k= 0.10:

Absolute clearance is 50.45 meters at 1.00 km from LEE.
Minimum clearance is 13.81 times the first Fresnel Zone
Radius at 42.00 GHz, and 15.00 km from LEE.

Table 2-4. (continued)

Terrain Profile and Ray Path Information (continued)
Lee Hill to Receiver Path

ANGLES OF ATMOSPHERIC PENETRATION:

For an Earth Radius Factor of k= 1.33:

Take off angle at LEE is -2.35 degrees.
Take off angle at RCV is 2.23 degrees.
Minimum angle of penetration is 2.23 degrees.

For an Earth Radius Factor of k= 0.10:

Take off angle at LEE is -3.06 degrees.
Take off angle at RCV is 1.51 degrees.
Minimum angle of penetration is 1.51 degrees.

PATH NOTES:

1. Mean atmospheric pressure on path is 79.32 kPa

2. Mean Path height for k=4/3 is 329.91 meters.

3. Has an allowance for growth been included in the tree heights shown on the profile?

5. The estimated annual worst month average snow depth at the location of minimum clearance is 1.00 m.

6. Additional comments: (entered by operator)

   This is a sample user comment

Table 2-5. Example of Antenna Height Output of the Terrain Profile and Ray Path Module

Antenna Calculations
Lee Hill to Receiver Path

To obtain 20.5 First Fresnel clearance(s) at an Earth Radius Factor of k= 1.3300 and a frequency of 42.00 GHz, the following antenna heights would be required:

Transmitter Ht (m)	Receiver Ht (m)	Min Clearance (m)	Distance from Lee Hill (km)
50.00	390.74	53.12	1.00
60.00	227.62	53.12	1.00
70.00	64.51	53.12	1.00
80.00	60.16	77.44	15.00
90.00	58.62	77.44	15.00
100.00	57.08	77.44	15.00

Table 2-6. Example Path Profile Output of the Terrain Profile and Ray Path Module

P r o f i l e D a t a
Lee Hill to Receiver Path

	Metric Units			English Units		
Point No.	Dist (km)	Elev (m)	Code Height (m)	Dist (mi)	Elev (ft)	Code Height (ft)
LEE	0.00	2284		0.00	7492	
1	1.00	2260		0.62	7416	
2	1.20	2169		0.75	7116	
3	1.80	2076		1.12	6810	
4	2.40	1983		1.49	6507	
5	3.00	1917		1.86	6289	
6	3.60	1922		2.24	6307	
7	4.20	1966	Tree 50	2.61	6451	Tree 164
8	5.00	1667		3.11	5469	
9	5.40	1796		3.36	5892	
10	6.00	1705		3.73	5594	
11	6.60	1691		4.10	5548	
12	7.20	1670		4.47	5478	
13	7.60	1657		4.72	5435	
14	8.40	1646		5.22	5402	
15	9.00	1650	Bldg 100	5.59	5412	Bldg 328
16	9.60	1650		5.97	5414	
17	10.20	1638		6.34	5373	
18	11.00	1617		6.84	5305	
19	12.00	1591		7.46	5220	
20	12.60	1587		7.83	5208	
21	13.20	1590	Water 20	8.20	5218	Water 66
22	13.80	1596		8.57	5237	
23	14.40	1601		8.95	5254	
24	15.00	1610	Obst 75	9.32	5282	Obst 246
25	15.60	1616		9.69	5303	
26	16.20	1610		10.07	5283	
27	17.00	1618		10.56	5310	
28	17.15	1614		10.66	5295	
29	17.31	1615		10.76	5299	
30	17.31	1616		10.76	5302	
RCV	17.31	1612		10.76	5289	

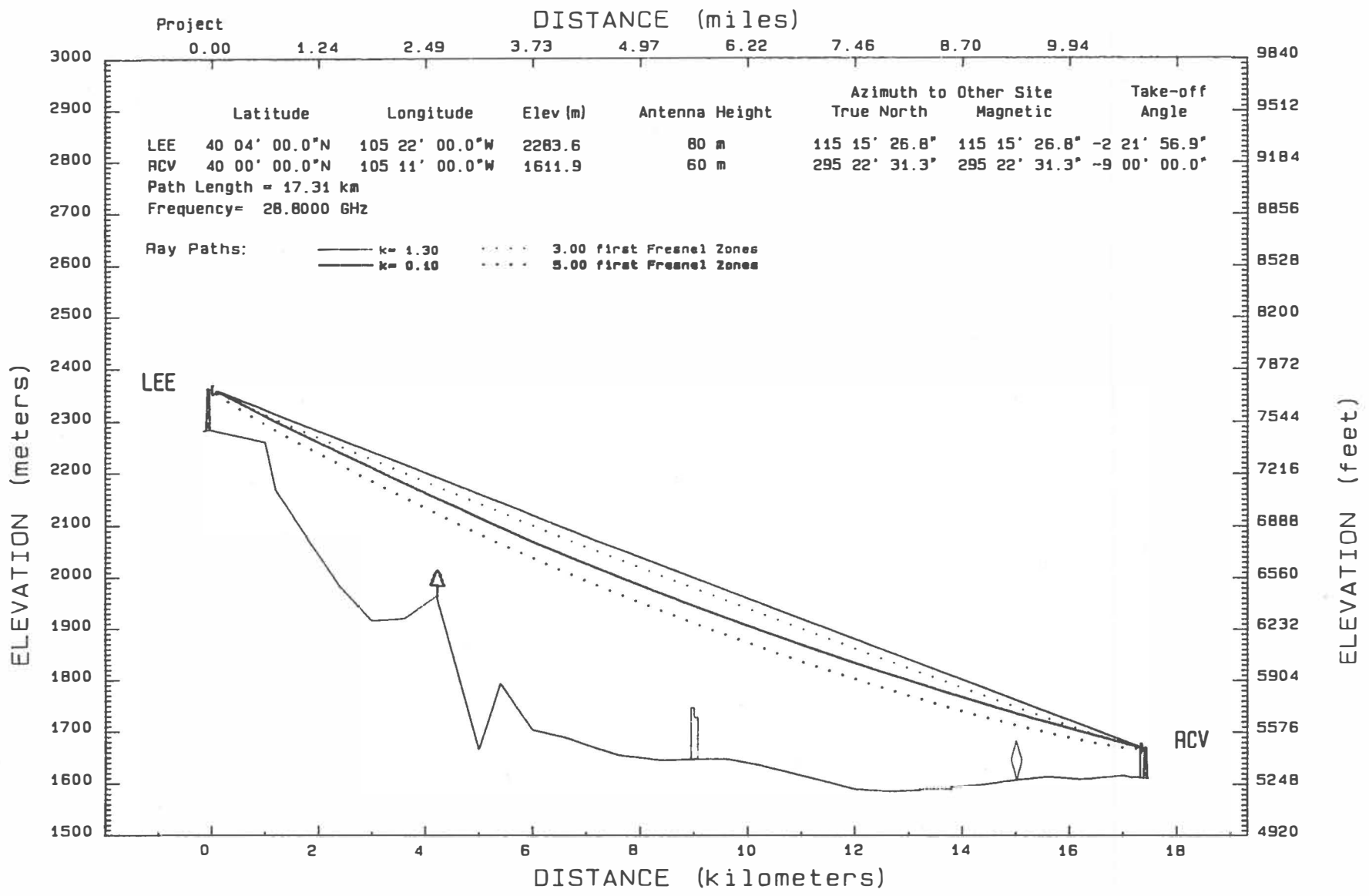

Figure 2-1. Example path profile and ray tracing plot of the terrain profile and ray path module.

3.1.1 Propagation effects modeled

Three propagation effects were modeled because together they essentially determine the levels of EHF transmission loss exceeded small percentages of the time (less than 10 percent of the time). These propagation effects are rain on path, multipath, and clear-air absorption by oxygen and water vapor.

Rain attenuation

Attenuation by rain on path is the most significant threat to EHF telecommunication availability. Transmission losses in excess of 200 dB may occur. The accurate prediction of rain attenuation is by far the most essential ingredient in predicting the availability of EHF telecommunication systems. For many paths, predictions based on rain attenuation alone would be sufficient, with the error resulting from excluding the other propagation effects being much less than the normal year-to-year variation in rain attenuation. Dispersive effects by rain do not merit modeling for bandwidths less than 1 GHz (Espeland et al, 1984).

Multipath

The severity of multipath varies widely from path to path but generally the narrow beamwidths achievable and the tendency toward shorter paths at EHF's would decrease the amount of multipath expected. On the other hand, the shorter wavelengths afford more opportunity for destructive interference. To date there is not enough experience to evaluate the significance of the contribution of multipath to the overall cumulative distribution of transmission loss on EHF paths. Because of this and because multipath can result in fades in excess of 40 dB, it has been included as one of the propagation phenomena modeled.

In addition to causing fades, multipath also causes amplitude and phase dispersion. This effect of multipath has not been included in ETSEM because the multipath delay times expected for short paths and narrow beamwidths do not cause enough distortion to merit modeling for bandwidths less than 50 MHz (Webster, 1983).

Frequency and space diversity improvement for multipath fading have not been included. Because rain attenuation is expected to account for essentially all the outage time of high reliability EHF systems, diversity is not a cost effective way of increasing availability.

Clear Air Absorption

Clear air absorption by oxygen and water vapor ranges from less than 0.1 dB/km to more than 15 dB/km depending on frequency (10 - 100 GHz). Because the contribution to the total cumulative distribution of transmission loss can be large, a

clear air attenuation model has been included in ETSEM. Clear air amplitude and phase dispersion do not need to be modeled for reasonable path lengths and bandwidths less than 5 GHz (Shanmugan et al, 1985).

3.1.2 Propagation effects not modeled

Clouds and Fog

Although it has been shown that attenuation by clouds can add significantly to the cumulative distribution of transmission loss on earth-space paths for frequencies above 30 GHz (Allen,1983), attenuation due to clouds and fog have not been included in ETSEM. For most terrestrial LOS-EHF paths, cloud and fog attenuation should not effect the availability statistics. In addition, there is not a model available at this time that predicts the cumulative distribution of attenuation due to fog (or clouds on path) for EHF as a function of path and climatological or geographic parameters.

However, there may exist paths in fog-prone areas such as parts of Germany or elevated paths between mountain tops that must penetrate a significant amount of cloud, for which the resulting attenuation does effect the availability statistics. It may be that fog and cloud models will need to be included in ETSEM at some future time for such paths, especially at the upper end of the 10 to 100 GHz frequency range.

Snow

Attenuation by snow is so much less than attenuation by rain (Espeland et al, 1984) that it does not need to be modeled for any path that is designed to operate reliably during intervals of time when rain is possible. For this reason attenuation by snow has not been included in ETSEM. Of course, snow attenuation sometimes should be considered for any path being designed to operate under conditions when rain is not possible or very unlikely and considerable snow is expected, such as winter months at high latitudes. However, snow is less of an attenuator than fog and therefore its threat to availability is not difficult to overcome in even the snowiest environment.

Obstruction Fading

Obstruction fading is caused by the k factor (effective Earth radius factor) becoming so small that, in effect, the Earth bulges up and blocks the path so that it is no longer LOS for the radio waves. Obstruction fading can occur for SHF and EHF links. It has not been included in ETSEM because a link designed with adequate Fresnel-zone clearance (for an effective earth's radius factor equal to 2/3) should not suffer obstruction fading. An obstruction fading model is available (Vigants, 1981; Schiavone, 1981).

Antenna Decoupling and Defocusing

Antenna decoupling occurs when the k factor changes enough to cause the angle of departure or arrival at the transmitting or receiving antennas to be outside the main lobe of the antenna pattern. These angles are the same for SHF and EHF radio waves; however, narrower beamwidths are more easily achieved for the shorter wavelength EHF waves. Appendix A shows that for beamwidths greater than about 0.04 deg per km of path length there should not be a decrease in availability due to antenna coupling. For beamwidths near this value some caution should be exercised by consulting Appendix A to determine if further investigation of the threat of antenna decoupling to the link is necessary.

Defocusing occurs when the refractive index gradient is structured along the path in such a way as to cause the antenna beam to fan out, reducing the amount of power arriving at the receiving antenna (Allen et al., 1982). Defocusing occurs for SHF and EHF frequencies. It should not affect availability but for an occasional problem path that is located near frequent and extreme atmospheric layering.

3.2 Rain Attenuation Module

There are three secondary models in the rain attenuation module. The first model predicts the cumulative distribution of point rain rate. The second model converts the cumulative distribution of rain rate into a cumulative distribution of attenuation for the path (point-to-path conversion) using the third model of raindrop size distribution.

An example of the tabular output of this module is given in Table 3-1. The graphical output is given in Figure 3-1.

3.2.1 Monthly point rain rate distribution

The model of point rain rate distribution developed by Rice and Holmberg (1973) was selected because it is the only model that gives the rain rate distribution in terms of commonly recorded climatological parameters. The Rice-Holmberg model gives the amount of time, T, in hours that the point rain rate, R, in mm/h is exceeded as

$$T = M \{0.03\beta\exp(-0.03R) + 0.2(1-\beta)[\exp(-0.258R) + 1.86\exp(-1.63R)]\} \quad (3\text{-}1)$$

where M is the total precipitation in mm for the time period and β is the thunderstorm ratio parameter that indicates what fraction of the rainfall is from convective storms. Because monthly predictions of performance are desirable for short-term tactical deployments, monthly distributions of rain rate are needed.

Table 3-1. Example Output of the Rain Attenuation Module

Distribution of Rain Attenuation
Lee Hill to Receiver Path

Time Period		Jun - Jun
Carrier Frequency	(GHz)	42.00
Path Length	(km)	17.31

Percent of Time Attenuation Exceeded	Time	Attenuation
10.0000 %	72.00 hr	0.00 dB
5.0000 %	36.00 hr	0.00 dB
2.0000 %	14.40 hr	0.00 dB
1.0000 %	7.20 hr	12.13 dB
0.5000 %	3.60 hr	21.75 dB
0.2000 %	1.44 hr	36.28 dB
0.1000 %	43.20 min	47.06 dB
0.0500 %	21.60 min	59.80 dB
0.0200 %	8.64 min	91.99 dB
0.0100 %	4.32 min	115.01 dB
0.0050 %	2.16 min	134.01 dB
0.0020 %	51.84 sec	155.46 dB
0.0010 %	25.92 sec	169.69 dB
0.0005 %	12.96 sec	182.99 dB
0.0002 %	5.18 sec	198.89 dB
0.0001 %	2.59 sec	210.37 dB

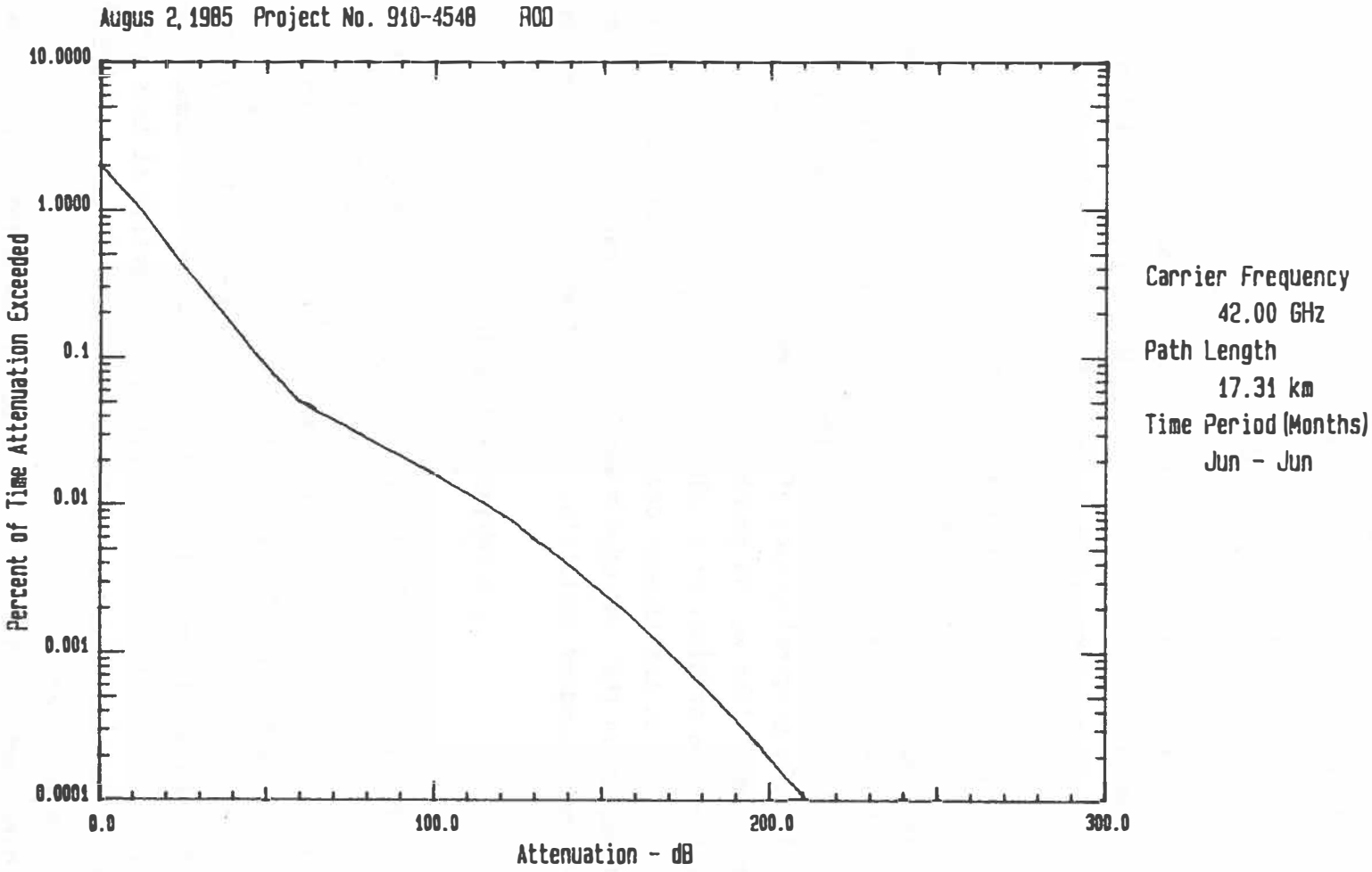

Figure 3-1. Example output of the rain attenuation module.

Unfortunately, the Rice-Holmberg model gives β as a function of yearly statistics so that its original form cannot be used to predict monthly cumulative distributions of point rain rate. An alternate formulation for β is needed.

Dutton (1984) used the intuitive formulation

$$\beta = U/D \tag{3-2}$$

where U is the mean number of days with thunderstorms and D is the mean number of days with more than 0.01 inches of rain. Since U and D are available monthly statistics, (3-2) is a usable formulation to predict monthly cumulative distributions of R.

However, the question arises of how good an estimate is (3-2). This question was addressed by taking 18 cities located in the United States (Allen et al, 1983) and computing the yearly β according to the original Rice-Holmberg model. Using these values as "true" values, yearly values were calculated using (3-2) and compared. The standard deviation of these later values about the original ones was 129 percent. If only original values of β greater than 0.15 (13 cases) were used then the standard deviation was 93 percent. Thus the β values given (3-2) differ significantly from the original Rice-Holmberg values.

It was noticed that the largest deviations occurred for cities with small M. Therefore a formulation that included M was tried with parameters that were adjusted to give the minimum standard deviation. The resulting formulation is given by

$$\beta = (M/1800 + 0.16)U/D. \tag{3-3}$$

The standard deviation for this later formulation was 43 percent for all 18 cities and 31 percent for the 13 cities that had original β greater than 0.15. Thus the β values given by (3-3) are in better agreement with the Rice-Holmberg values than the values using Dutton's formulation (3-2).

Because rain is of utmost importance to EHF system availability futher study is indicated for the development of an estimate of β that uses commonly available monthly climatological statistics. Although it is uncertain at this time which formulation for β is best, Equation (3-3) was selected for use in ETSEM.

3.2.2 Point to path conversion

A model developed by Crane (1980) is used for the point-to-path conversion of the point rain rate. This model was chosen because it is widely known, used by the CCIR, not too complex, and has been shown by Dutton (1984) to be one of the better models.

Crane's algorithm, as used in ETSEM, to find the attenuation exceeded P percent of the time is given in the following steps:

1. Determine if the path length, D, is greater than 22.5 km. If so, the modified point rain rate, R', for the modified percentage of time

$$P' = P(22.5/D) \tag{3-4}$$

and a path length of 22.5 km are used for subsequent calculations. Otherwise the original path length and the original point rain rate exceeded P percent of the time are used. R is found iteratively from (3-1) for the T corresponding to the appropriate percentage of time.

2. The following are then computed:

$$b = 2.3\ R^{-0.17} \tag{3-5}$$

$$c = 0.026 - 0.03 \ln R \tag{3-6}$$

$$d = 3.8 - 0.6 \ln R \tag{3-7}$$

$$u = (cd + \ln b)/d. \tag{3-8}$$

3. Finally the attenuation, A, exceeded P percent of the time is computed. If $d < D$, then

$$A = \alpha R^{\beta} \left[\frac{e^{u\beta d} - 1}{u\beta} - \frac{b^{\beta} e^{c\beta d}}{c\beta} + \frac{b^{\beta} e^{c\beta D}}{c\beta} \right] \tag{3-9}$$

otherwise ($d \geq D$)

$$A = \alpha R^{\beta} \left[\frac{e^{u\beta D} - 1}{u\beta} \right] \tag{3-10}$$

where α and β are parameters that depend on the raindrop size distribution to be discussed in the next section.

3.2.3 Drop-size distribution

It is usual to model the specific attenuation through rain by

$$A = \alpha R^{\beta} \tag{3-11}$$

where α and β depend on the distribution of drop sizes and on the radio wave frequency. Tables of these parameters have been computed by Olsen, Rogers, and Hodge (1978) for several of the more popular raindrop size distributions.

The author compared measurements of the ratio of rain attenuation for 11.4 and 28.8 GHz made on a 27 km path in Colorado (Espeland et al, 1984) with the ratio of attenuation that would be expected for the different drop-size distributions using the parameters computed by Olsen et al. The ratios predicted for the distribution given by Joss, Thams, and Waldvogel (1968) for thunderstorms agreed best with the measured ratios. The parameters of Dutton et al (1983) that are given for five climate regions and were derived from a survey of measured drop size distributions were also compared with the parameters of Olsen et al. Again the Joss thunderstorm parameters showed the closest agreement, falling in about the middle of the range of values. Therefore the α and β parameters for the Joss distribution are used in ETSEM for (3-11). This distribution also seems to be a good choice when it is realized that for many locations thunderstorms produce the high rain rates that are a threat to high availability links.

There is a range of more than a factor of 2 in EHF specific attenuation for the different drop size distributions used by Olsen et al and a range of a factor of 4 for the different climate regions used by Dutton et al. Thus there is a great uncertainty in EHF specific attenuation. This uncertainty is the most critical limitation to reliable prediction of EHF system availability and is therefore the area of most pressing need for further research. It could well be that drop-size distributions dependent upon climate or type of rain will need to be developed before dependable predictions of the cumulative distributions of EHF attenuation can be made.

3.3 Clear-Air Absorption Module

The model of clear-air absorption can be broken into two parts. The first part is due to molecular oxygen and varies with time by only a few percent in dB. In the range of 10 to 100 GHz the absorption peaks at about 15 dB/km near 60 GHz and decreases to less than 0.1 dB/km outside the range of approximately 45 to 75 GHz.

The second part is due to water vapor and accordingly varies widely with time, season, and climate. Except for a slight increase near 22 GHz the absorption increases from about 0.01 dB/km/g/m^3 at 10 GHz to nearly 0.1 dB/km/g/m^3 at 100 GHz in the lower atmosphere. At 22 GHz the absorption is approximately 0.04 dB/km/g/m^3. Since the water vapor content of the atmosphere can exceed 50 g/m^3, the attenuation at 100 GHz can be greater than 5 dB/km.

An example of the tabular output of this module is given in Table 3-2. The graphical output is given in Figure 3-2.

3.3.1 Oxygen Absorption

Oxygen absorption for frequencies between 10 and 100 GHz can be accurately

Table 3-2. Example Output of the Clear-Air Absorption Module

Distribution of Clear Air Absorption
Lee Hill to Receiver Path

Time Period		Jun - Jun
Carrier Frequency	(GHz)	42.000
Path Length	(km)	17.31
Median Absorption	(dB)	1.98

Percent of Time Attenuation Exceeded	Time	Attenuation
10.0000 %	72.00 hr	1.98 dB
5.0000 %	36.00 hr	1.98 dB
2.0000 %	14.40 hr	2.26 dB
1.0000 %	7.20 hr	2.26 dB
0.5000 %	3.60 hr	2.41 dB
0.2000 %	1.44 hr	2.75 dB
0.1000 %	43.20 min	2.75 dB
0.0500 %	21.60 min	2.75 dB
0.0200 %	8.64 min	2.94 dB
0.0100 %	4.32 min	3.13 dB
0.0050 %	2.16 min	3.13 dB
0.0020 %	51.84 sec	3.34 dB
0.0010 %	25.92 sec	3.34 dB
0.0005 %	12.96 sec	3.57 dB
0.0002 %	5.18 sec	3.57 dB
0.0001 %	2.59 sec	3.80 dB

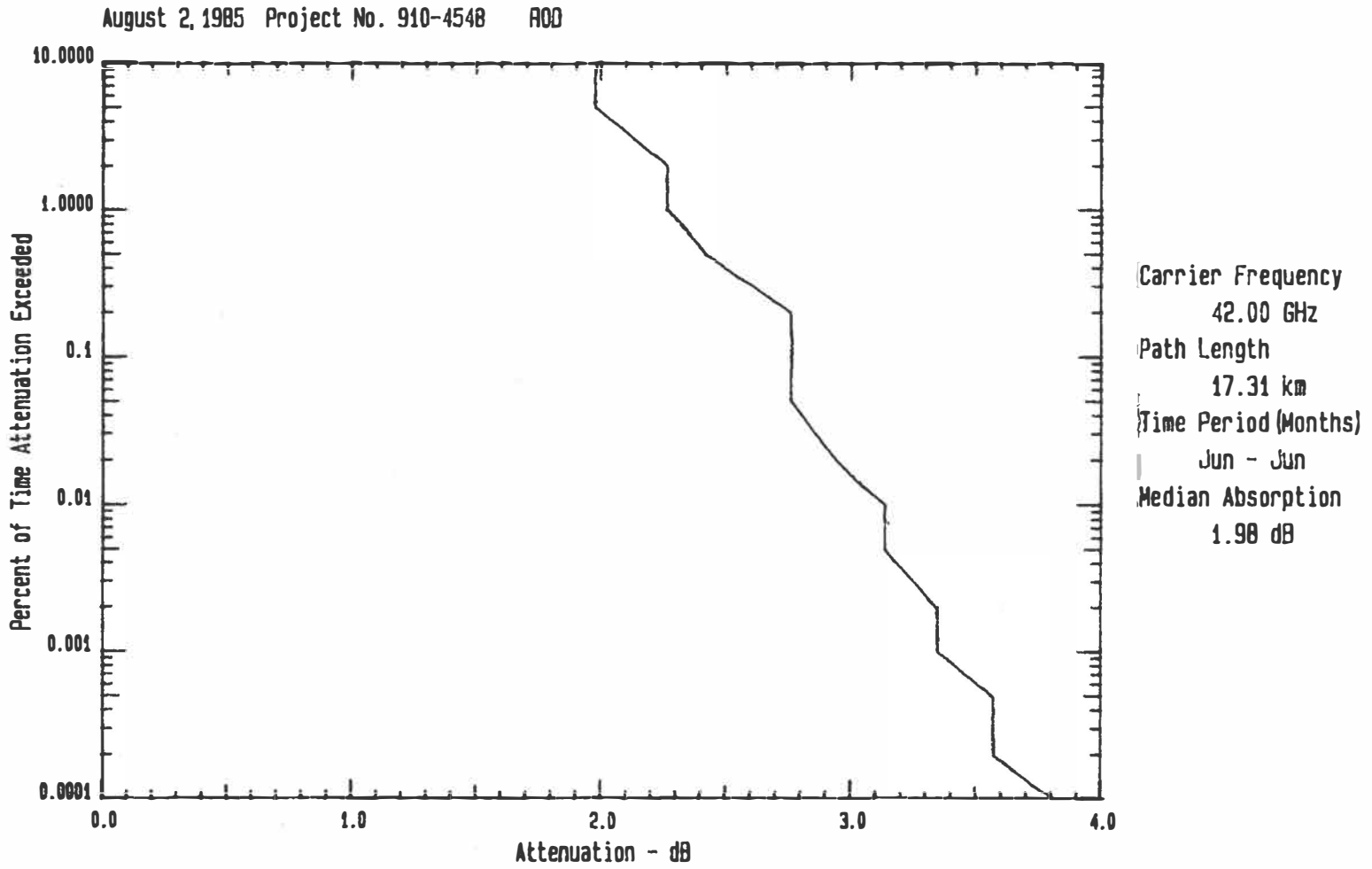

Clear Air Absorption Distribution
Lee Hill to Receiver Path

Figure 3-2. Example output of the clear-air absorption module.

modeled as the sum of more than 40 resonant absorption lines around 60 GHz and a nonresonant continuum (Liebe, 1983). This type of modeling is computation intensive, involving the summation of over 40 line contributions, and would require a prohibitive amount of computation time for ETSEM. A simpler model good for altitudes below 4,570 m (15,000 ft) that requires approximately two orders of magnitude less computation time was developed.

The model is an expansion in pressure and temperature of the specific attenuation with parameters that are frequency dependent contained in a table. The expansion for the specific attenuation, α, in dB/km is

$$\alpha = a\,\theta^{\beta_1} P^{\beta_2} \exp(\beta_3\theta^2 + \beta_4\theta^2 P) \qquad (3\text{-}12)$$

where P is pressure and θ is the relative inverse temperature given by $\theta = 300/T$ with T in degrees Kelvin. The a, β_1, β_2, β_3, and β_4 are parameters interpolated in frequency from the table (see Appendix B). These parameters were found by fitting oxygen absorption predictions (Liebe, 1983) for frequencies from 10 to 100 GHz. When the parameters are interpolated from the table, (3-12) gives specific attenuations that agree within 6.5 percent of those of Liebe.

3.3.2 Water vapor absorption

The specific water vapor absorption model for frequencies from 10 to 100 GHz is simple. It consists of a water vapor continuum (Liebe, 1983) and a single line at 22 GHz using a Lorentz line shape. The specific water vapor absorption, α, in dB/km is given by

$$\alpha = 0.1820 f N'' \qquad (3\text{-}13)$$

where f is frequency in GHz and N" is the imaginary part of the complex refractive index. Now

$$N'' = N_l'' + N_c'' \qquad (3\text{-}14)$$

where N_l'' is the contribution by the 22 GHz line and N_c'' is the contribution of the water vapor continuum (due to higher frequency lines).

Using the Lorentz line shape,

$$N_l'' = S\gamma^2/[(\nu_0 - f)^2 + \gamma^2] \qquad (3\text{-}15)$$

where

$$S = 0.112\ e\ \theta^{3.5} \exp[2.143(1 - \theta)] \tag{3-16}$$

$$\gamma = 28.1\ (P\ \theta^{0.8} + 4.8\ e\ \theta)\ 10^{-3} \tag{3-17}$$

$$\nu_0 = 22.23508 \tag{3-18}$$

and e is the partial water vapor pressure in kPa.

The water vapor continuum is given by

$$N''_c = [1.4\ e\ P\ \theta^{2.5} + 54.1\ e^2 \theta^{3.5}]\ f\ 10^{-6}. \tag{3-19}$$

3.3.3 Cumulative distribution of absorption

The clear-air specific absorption is modeled in ETSEM as the sum of a constant dry-air term and a random water-vapor term for each month. This is a reasonable approach since the absorption by oxygen only varies by a few percent during a given month while the absorption by water vapor varies by a much larger percentage for most locations.

The constant for dry-air attenuation is found from the mean temperature and pressure for the month.

Bean and Cahoon (1957) modeled the cumulative distribution of absolute humidity in g/m^3 by giving the humidity exceeded 90, 95, and 99 percent of the month in terms of the mean absolute humidity for the month. It was found that these levels corresponded closely to the levels that would be exceeded for a normally distributed random absolute humidity with standard deviation

$$\sigma = 0.0094\overline{\rho} + 2.05 \tag{3-20}$$

where $\overline{\rho}$ is the mean absolute humidity for the month in g/m^3 (see Appendix C). Thus, the absolute humidity was modeled as a normally distributed random variable with standard deviation as given in (3-20).

To find the specific absorption exceeded P percent of a month from the mean atmospheric pressure, p', mean relative humidity, RH, and mean relative inverse temperature, θ, the following steps are used:

1. The mean water vapor pressure and absolute humidity are found from

$$e_s = 2.409\ \theta^5\ 10^{(10-9.834\theta)} \tag{3-21}$$

$$\overline{e} = e_s \overline{RH}/100 \tag{3-22}$$

and

$$\rho = 7.217\ \overline{e}\ \theta. \tag{3-23}$$

2. The dry air pressure is found from

$$p = p' - e. \tag{3-24}$$

3. The absolute humidity exceeded P percent of the month is found by solving

$$P(\rho) = 100\{1 - \text{erf}\,[(\rho - \bar{\rho})/\sigma\sqrt{2}]\}/2 \qquad (3\text{-}25)$$

for ρ iteratively where the value of the error function, erf, is found from the expansion given in Abramowitz and Stegun (1964)

$$\text{erf}(x) = 1 - (a_1 t + a_2 t^2 + a_3 t^3 + a_4 t^4 + a_5 t^5)\exp(-x^2) \qquad (3\text{-}26)$$

where

$$t = (1 + 0.3275911x) \qquad (3\text{-}27)$$
$$a_1 = 0.254829592 \qquad (3\text{-}28)$$
$$a_2 = -0.284496736 \qquad (3\text{-}29)$$
$$a_3 = 1.421413741 \qquad (3\text{-}30)$$
$$a_4 = -1.453152027 \qquad (3\text{-}31)$$
$$a_5 = 1.061405429. \qquad (3\text{-}32)$$

4. The ρ found above is converted back into kPa using

$$e = \rho/7.217\ \theta. \qquad (3\text{-}33)$$

5. The absorption by water vapor exceeded P percent of the month is then obtained from the vapor pressure, e, the dry air pressure p, and the relative inverse temperature, θ, using (3-13) through (3-19).
6. The dry air attenuation is obtained from the dry air pressure and relative inverse temperature using (3-12).
7. The attenuation by water vapor and dry air are summed to give the absorption exceeded P percent of the month.

3.4 Multipath Fading Module

The multipath fading model of Crombie (1983) was chosen for use in ETSEM. Crombie's model was developed specifically for frequencies above 10 GHz and, for the data base used to develop the model, the standard error of the estimated probability of multipath fading greater than 20 dB was 80 times smaller than that for the more widely known model of Barnett (1972) used in ADSEM.

Like the Barnett model, Crombie's model is a worst month model. The author does not know of any method for scaling from the worst month to the other months of the year. Thus the model would be expected to normally overpredict the amount of multipath fading for an arbitrary interval of months. This is the greatest apparent

shortcoming of the model at this time.

The formulation of Crombie's model selected for ETSEM gives the percent, P, of the worst month that multipath attenuation, A, is exceeded as

$$P(A) = 100 \times 10^{(-A/10-0.997)} \times d^{2.49} \times f^{0.84} \times \theta^{1.19} \times h^{-2.44} \qquad (3\text{-}35)$$

where

d = path length (km),

f = frequency (GHz),

$\theta = \sqrt{\theta_T \cdot \theta_R}$,

h = average height at center of path (m),

θ_T = beamwidth of transmitting antenna (mr), and

θ_R = beamwidth of receiving antenna (mr).

An example of the tabular output of this module is given in Table 3-3. The graphical output is given in Figure 3-3.

3.5 Combined Cumulative Distribution Module

Once the cumulative distributions for the three propagation effects are determined, it is necessary to estimate the overall cumulative distribution of the RSL from them in order to predict the availability of the communication system.

Because the attenuation due to water vapor associated with rain can be quite significant, the water vapor and rain attenuation distributions were added together by adding the attenuations exceeded each percentage of the year. For example, to estimate the attenuation exceeded 1 percent of the time by the combined effects of rain and water vapor, the attenuation by rain exceeded 1 percent of the time is added to the attenuation by water vapor exceeded 1 percent of the time.

To find the total cumulative distribution of attenuation, the combined rain and water vapor attenuation distribution is combined with the multipath attenuation distribution. Because rain and multipath fading usually occur at different times, the distributions are combined by adding the amount of time each attenuation level is exceeded in each distribution. For example, the amount of time that 10 dB attenuation is exceeded for the total cumulative distribution is found by adding together the amount of time that multipath attenuation exceeds 10 dB and the amount of time that the combined rain and water vapor attenuation exceeds 10 dB.

The combined cumulative distribution of attenuation is used with the link gain discussed in section 4.2 to compute the cumulative distribution of received signal level (RSL). In Figure 3-4 an example of the graphical output of the RSL distribution is shown. In Table 3-4 the tabular output is given.

Table 3-3. Example Output of the Multipath Attenuation Module

Distribution of Multipath Attenuation
Lee Hill to Receiver Path

Time Period		Jun - Jun
Carrier Frequency	(GHz)	42.00
Path Length	(km)	17.31
Min. Ray Height at Mid Path	(m)	226.2
Transmitter Beamwidth	(degrees)	0.50
Receiver Beamwidth	(degrees)	0.50

Percent of Time Attenuation Exceeded	Time	Attenuation
10.0000 %	72.00 hr	0.00 dB
5.0000 %	36.00 hr	0.00 dB
2.0000 %	14.40 hr	0.00 dB
1.0000 %	7.20 hr	0.00 dB
0.5000 %	3.60 hr	0.00 dB
0.2000 %	1.44 hr	0.00 dB
0.1000 %	43.20 min	0.00 dB
0.0500 %	21.60 min	1.28 dB
0.0200 %	8.64 min	5.26 dB
0.0100 %	4.32 min	8.27 dB
0.0050 %	2.16 min	11.28 dB
0.0020 %	51.84 sec	15.26 dB
0.0010 %	25.92 sec	18.27 dB
0.0005 %	12.96 sec	21.28 dB
0.0002 %	5.18 sec	25.26 dB
0.0001 %	2.59 sec	28.27 dB

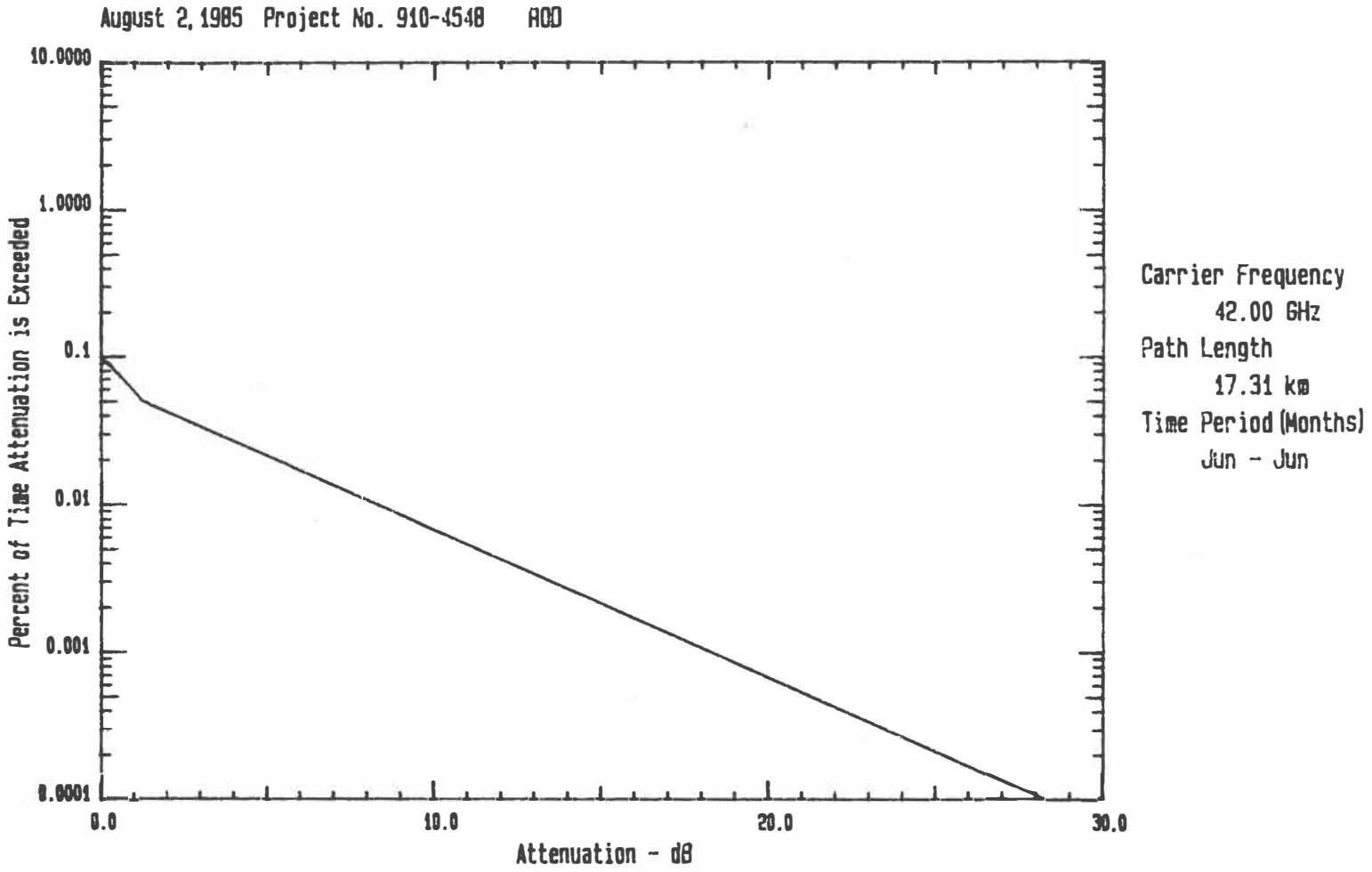

Figure 3-3. Example output of the multipath attenuation module.

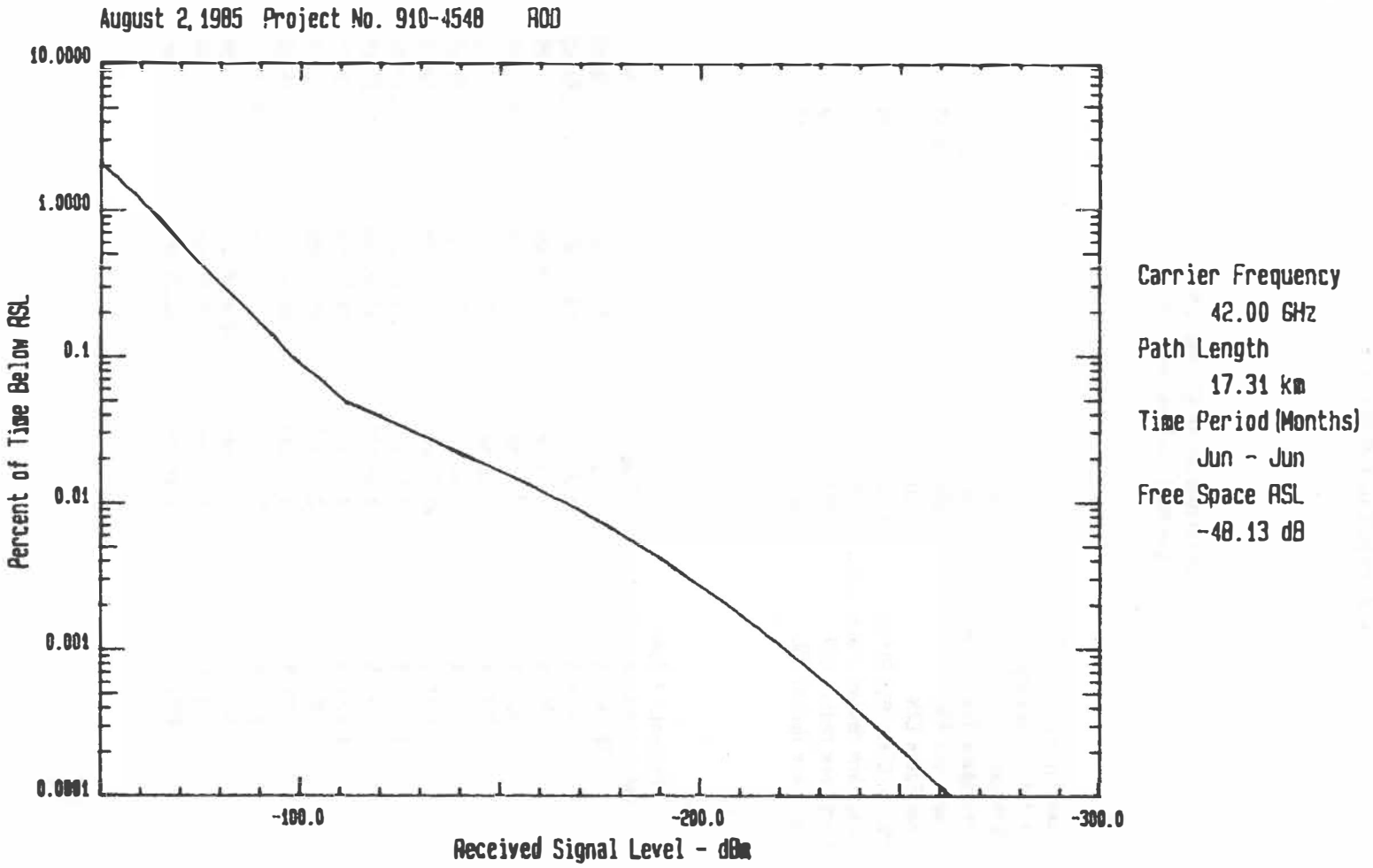

Received Signal Level Distribution
Lee Hill to Receiver Path

Figure 3-4. Example output of the combined distribution module.

Table 3-4. Example Output of the Combined Distribution Module

Distribution of RSL and C/N
Lee Hill to Receiver Path

Time Period		Jun - Jun
Carrier Frequency	(GHz)	42.000
Path Length	(km)	17.31
Free Space Trans. Loss	(dB)	149.68
Free Space RSL	(dBm)	-48.13
Free Space C/N	(dB)	42.86
Median Clear Air Atten.	(dB)	1.98
Long-term Median Trans. Loss	(dB)	151.66
Long-term Median C/N	(dB)	40.88
Long-term Median RSL	(dBm)	-50.11

Percent of Time Below Indicated RSL	Time	RSL	C/N
10.0426 %	72.31 hr	-50.11 dBm	40.88 dB
5.0426 %	36.31 hr	-50.11 dBm	40.88 dB
2.0399 %	14.69 hr	-50.39 dBm	40.60 dB
1.0024 %	7.22 hr	-62.52 dBm	28.47 dB
0.5003 %	3.60 hr	-72.29 dBm	18.70 dB
0.2000 %	1.44 hr	-87.17 dBm	3.82 dB
0.1000 %	43.20 min	-97.95 dBm	-6.96 dB
0.0500 %	21.60 min	-110.68 dBm	-19.69 dB
0.0200 %	8.64 min	-143.06 dBm	-52.07 dB
0.0100 %	4.32 min	-166.28 dBm	-75.29 dB
0.0050 %	2.16 min	-185.28 dBm	-94.29 dB
0.0020 %	51.84 sec	-206.94 dBm	-115.95 dB
0.0010 %	25.92 sec	-221.17 dBm	-130.18 dB
0.0005 %	12.96 sec	-234.68 dBm	-143.70 dB
0.0002 %	5.18 sec	-250.59 dBm	-159.60 dB
0.0001 %	2.59 sec	-262.30 dBm	-171.31 dB

3.6 Climatological Data Bases

The user of the model may input all the climatological parameters needed by the individual propagation models or may have them taken from the climatological data bases for North America and Europe included with the model.

The data bases contain the latitude, longitude and mean atmospheric pressure for selected meteorological observation stations and monthly mean statistics of:

- atmospheric temperature
- relative humidity or water vapor pressure
- total precipitation
- number of days with greater than 0.01 inch (or 0.25 mm) of precipitation
- number of days with thunderstorms

Data from 132 and 150 stations are included in the North American and European data bases respectively (Wallen, 1970 and 1977; Bryson and Hare, 1974).

When the data bases are used, the averages of the transmitter and receiver latitude and longitude are computed to estimate the latitude and longitude of the center of the path. These latitude and longitude are then used to "interpolate" from the data base.

The interpolation is done with the following procedure where all distances are measured in degrees as the square root of the sum of the squares of the difference in latitude and longitude.

1. The data base is searched for the closest two stations in each quadrant about the center of the path. Only stations within 8 deg latitude and longitude are considered.
2. For each meteorological parameter a weighted least squares fit is made using the weights $1/r$ or 1 if $r < 1$ where r is the distance of the station from the center of the path. If there are six to eight stations, a second-order bivariate polynomial (six unknowns) is fit on longitude and latitude. A first-order polynomial (three unknowns) is used if there are only three to five stations. For one to two stations the value of the parameter for the closest station is used.

This method of interpolating from the data bases was selected because of its simplicity. The weighting, order of the polynomial, and maximum distance of stations

from the path were all examined and selected to give the minimum standard error when interpolating mean monthly precipitation.

4. SYSTEM PERFORMANCE MODELS

4.1 Introduction

In order to predict the performance of a communication system the cumulative distribution of the RSL levle is used. It is determined from the cumulative distribution of transmission loss and the equipment gain. Models of the communication equipment performance as determined by the RSL are then used to predict the signal-to-noise ratio for analog (FM/FDM) systems and the bit error rate for digital systems.

4.2 Link Equipment Gain Module

The purpose of this module is to provide input to the program about the radio frequency equipment and to compute basic system parameters such as the antenna gains and free space RSL. The output of this module is tabular and an example is given in Table 4-1.

4.2.1 Inputs to Module

The following parameters are required input:

1. polarization
2. transmitter antenna diameter (parabolic assumed)
3. receiver antenna diameter
4. transmission line loss
5. diplexer and power splitter losses
6. receiver noise figure
7. receiver bandwidth
8. transmitter power.

4.2.2 Computed output of module

Free space transmission loss:

The free space transmission loss is calculated as

$$L_{fs} = 92.45 + 20 \log_{10}(fD) \qquad (4\text{-}1)$$

where f is the frequency in GHz and D is the path length in km.

Antenna gains and beamwidths:

The antenna gains for parabolic antennas are calculated as

$$G = 10 \log_{10}(\eta\pi^2 d^2/\lambda^2) \ \text{dBi} \qquad (4\text{-}2)$$

where η = aperture efficiency = 0.55

d = antenna diameter

Table 4-1. Example Output of the Link Equipment Gain Module

Equipment Parameters
Lee Hill to Receiver Path

Polarization			Vertical
Carrier Frequency	(GHz)		42.0
Path Length	(km)		17.3
		Transmitter	Receiver
Antenna Diameter	(Meters)	1.0	1.0
Antenna Gain	(dB)	50.3	50.3
Antenna Beam Width	(Degrees)	0.5	0.5
Transmission Line Type		ew71	ew71
Transmission Line Length	(Meters)	50.0	50.0
Line Loss per 100 meters	(dB)	2.0	2.0
Total Line Loss	(dB)	1.0	0.0
Circulator/Diplexer Loss	(dB)	5.0	5.0
Receiver Front-end Type			Mixer
Receiver Front-end Location			Antenna
Receiver Noise Figure	(dB)		10.0
Receiver Bandwidth	(MHz)		20.0
Transmitter Power	(dBm)		12.0
Free Space Trans Loss	(dB)		149.7
Free Space RSL	(dBm)		-48.1
Free Space C/N	(dB)		42.9

λ = wavelength (same units as antenna diameter).

The antenna beamwidths for parabolic antennas are calculated using

$$B = 10^{(2.215 - G/20)} \quad \text{deg} \tag{4-3}$$

where G is the antenna gain in dBi.

Free space RSL:

The free space RSL, S, is computed using

$$S = P_t + G_t + G_r - L_{tl} - L_d - L_{fs} \quad \text{dBm} \tag{4-4}$$

Where P_t = transmitter power in dBm

G_t = transmitter antenna gain in dBi

G_r = receiver antenna gain in dBi

L_{tl} = transmission line (feeder) loss in dB

L_d = diplexer, filter, and power splitter losses in dB

L_{fs} = free space transmission loss.

Free space C/N:

The free space carrier-to-noise ratio (C/N) is computed using

$$C/N = S + 168 - 10 \log_{10}(B) - F \quad \text{dB} \tag{4-5}$$

where S = free space RSL in dBm

B = the narrowest carrier or IF filter bandwidth in MHz

F = receiver noise figure in dB.

4.3 Analog Modulation Performance Modules

There are two analog modulation performance modules. The purpose of the first module is to compute the FM/FDM single-receiver transfer characteristic. The purpose of the second is to compute the availability of an FM/FDM system.

4.3.1 FM/FDM single-receiver transfer characteristic

The quality of the FM/FDM system is evaluated in terms of the S/N in the worst channel (usually the highest baseband channel). From equipment parameters input by the user, noise components are calculated and added together to compute the worst-voice-channel S/N as a function of the RSL (transfer characteristic). The noise components and other system parameters are included in the tabular output of this module, an example of which is given in Table 4-2. An example of the graphical output of the transfer characteristic is given in Figure 4-1.

Noise Sources:

In general, the noise sources are thermal noise, (receiver front end noise), echo noise (echo-delayed signals due to transmission line impedance mismatched), and nonlinear noise (distortion due to nonlinearities in the modulator or demodulator

Table 4-2. Example Output of the FM/FDM Single-Receiver Transfer Characteristic Module

Single Receiver Transfer Characteristic Parameters
Lee Hill to Receiver Path

System Type			FM/FDM
Polarization			Vertical
Carrier Frequency	(GHz)		42.0
Path Length	(km)		17.3
		Transmitter	Receiver
Antenna Gain	(dB)	50.3	50.3
Antenna Beam Width	(Degrees)	0.5	0.5
Transmission Line Length	(Meters)	50.0	50.0
Total Line Loss	(dB)	1.0	0.0
Feeder Velocity Ratio	(Percent)	61.00	61.00
VSWR at Antenna		1.06	1.06
VSWR at Radio		1.06	1.06
Return Loss at Antenna	(dB)	30.71	30.71
Return Loss at Radio	(dB)	30.71	30.71
Echo Delay Time (tau)	(micro s)	0.55	0.55
Echo Velocity (V)	(m/s)	183000.00	183000.00
Angle Delay	(Radians)	8.58	8.58
Signal to Echo Ratio (r)	(dB)	63.43	61.43
Parameter A		0.62	0.62
(S/D)-r	(dB)	2.11	2.11
S/D	(dB)	65.54	63.54
Feeder Echo S/N	(dB)	80.64	78.64

Table 4-2. (continued)

Single Receiver Tra s e haracteristic Parameters
Lee Hill to Receiver Path

Receiver Noise Figure	(dB)	10.0
Receiver IF Bandwidth	(kHz)	19660.1
Emphasis Improvment	(dB)	4.0
Number of Voice Channels		600
Voice Channel Bandwidth	(kHz)	3.1
Equipment NPR	(dB)	55.0
Peak Carrier Deviation	(kHz)	7330.0
RMS Per Channel Deviation	(kHz)	200.0
Threshold Extention		Yes
FM Threshold [P(FMTH)]	(dBm)	-88.1
P(FMTH) - P(TH)	(dB)	3.0
Thermal Noise Threshold [P(TH)]	(dBm)	-91.1
Baseband Signal Peak Factor		13.5
RMS Noise Loading Factor		17.8
Equipment Noise S/N	(dB)	66.1
Highest Modulating Frequency in BB	(kHz)	2500.0
Lowest Modulating Frequency in BB	(kHz)	100.0
Baseband Bandwidth	(kHz)	2400.0
Thermal S/N - C/N	(dB)	20.1
Thermal Noise for P(FMTH)	(pW0)	5000831.6
Equipment Noise	(pW0)	245.1
Total Feeder Echo Noise	(pW0)	22.3
Worst Channel S/N for P(FMTH)	(dB)	23.0
Long-Term Median C/N	(dB)	40.88
Long-Term Median RSL	(dBm)	-50.11
Thermal Noise for Med RSL	(pW0)	800.5

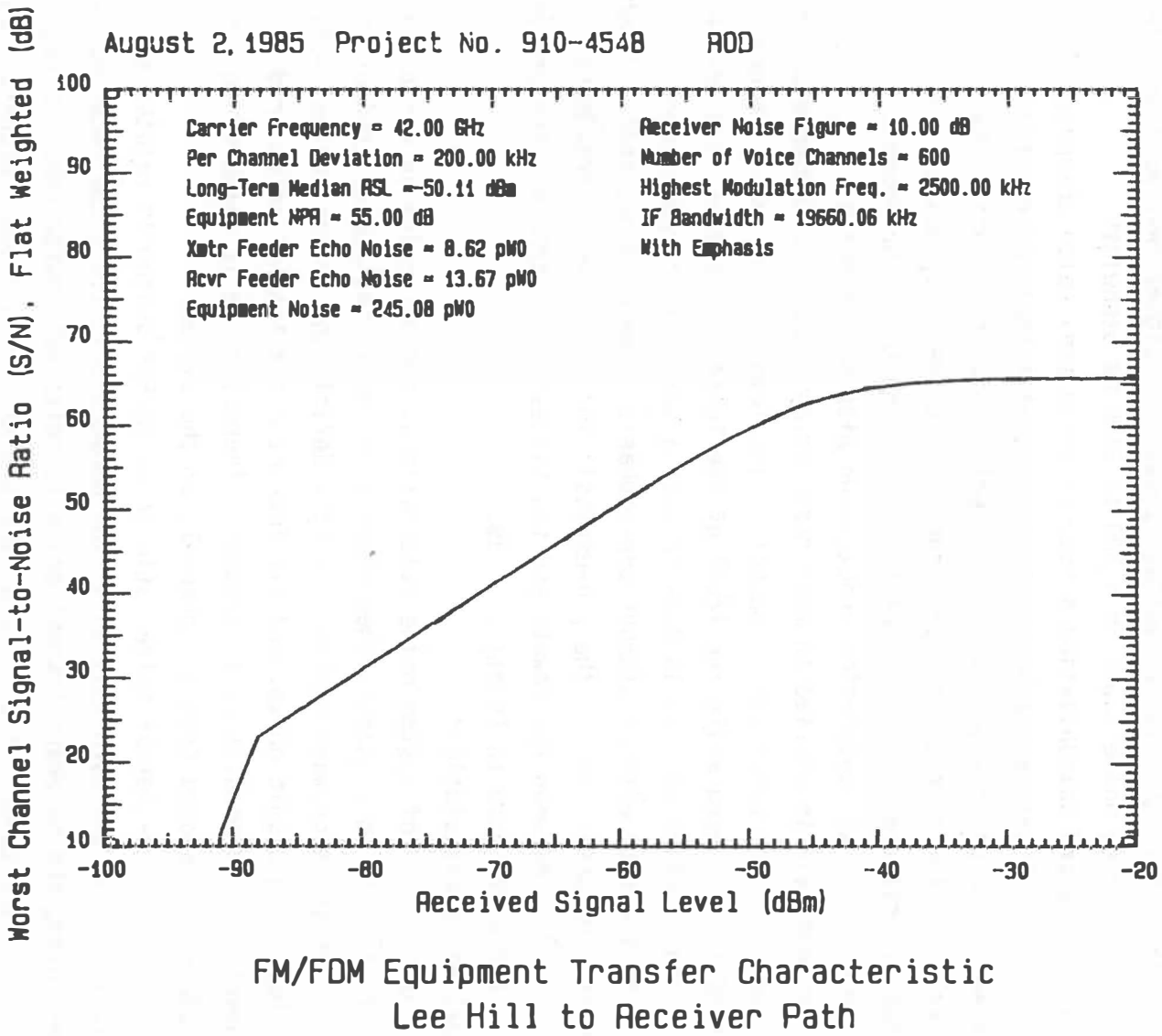

FM/FDM Equipment Transfer Characteristic
Lee Hill to Receiver Path

Figure 4-1. Example output of the FM/FDM single-receiver transfer characteristic module.

and multipath effects). The sum of the total feeder echo noise and equipment intermodulation noise is called the time invariant noise since these noise components do not depend on path loss variability. This time invariant noise is normally the dominant contribution for the relatively high signal levels near the long-term median RSL for which the thermal noise is normally low.

The most significant parameter influencing radio link design is the voice channel S/N. It is defined as 10 times the common logarithm of the ratio of an RMS single-tone signal power (usually 1000 Hz and at such a level that the sine-wave voltage peaks are roughly equal to the voltage peaks in a signal developed by a telephone talker) to average noise power in a 300 to 3400 Hz bandwidth.

In a wideband communication system in which many voice channels are frequency-division multiplexed into a baseband signal that extends over a large spectrum, it is necessary to be able to analyze the performance of any voice channel in the band. However, only the channel occupying the highest frequency position in the baseband is usually analyzed since its quality is expected to be the poorest of the channels because of its lower modulation index, even with pre-emphasis.

Pre-emphasis is applied in most radio-relay systems to compensate for the higher noise power in the upper voice channels. The level of the upper frequencies of the baseband is increased while the level of the lower frequencies is decreased before modulation is effected. It is done in such a way that the mean power of the baseband signal is the same with or without pre-emphasis. The CCIR has standardized the frequency characteristic of the pre-emphasis for all types of broadband systems (CCIR, 1982). Between the lowest and the highest voice channel, the pre-emphasis (i.e., the difference in level) is 8 dB.

Thermal Noise Calculation:

For purposes of system noise calculations, thermal noise is defined as noise from all sources in a channel when there is no modulated signal present on any of the channels in the microwave system. By this definition, thermal noise includes atmospheric and cosmic noise, and all intrinsic and thermal noise produced in the equipment when no modulation is present. Thermal noise is measured in a channel with all modulation removed from all channels of the system.

The signal-to-thermal noise ratio in an FM/FDM system is related to path loss variability. As the path loss on a link becomes low, i.e., the received signal level becomes high, the baseband thermal noise is relatively quite low. As received signal level decreases toward FM threshold, the thermal noise becomes higher. Signal-to-thermal noise ratio, S/N_t, in a voice channel is proportional to received signal level, P_r, or carrier-to-noise ratio, C/N. In the region above FM threshold, S/N_t may be expressed in several forms (Dept. of Defense, 1977b, p. 4-334), for example:

$$S/N_t = P_r + 20 \log_{10} \frac{\delta f}{f_m} - 10 \log_{10}(kTb_c \times 10^3) - F + I_E \quad (4\text{-}6)$$

$$S/N_t = C/N + 20 \log_{10} \frac{\delta f}{f_m} + 10 \log_{10} \frac{B_{IF}}{b_c} + I_E \quad (4\text{-}7)$$

$$\Delta F = (\delta f)\ (10^{PF/20})\ (10^{LF/20}) \quad \text{kHz} \quad (4\text{-}8)$$

$$LF = -10 + \log_{10}(n) \quad \text{dB} \quad (4\text{-}9)$$

where P_r = received carrier level in dBm

δf = rms per channel deviation in kHz

f_m = highest modulating frequency in the baseband in kHz

k = Boltzman's constant, 1.3804×10^{-20} milliJoules/K

T = antenna temperature taken to be 290 K

b_c = usable voice channel bandwidth taken to be 3.100 kHz

F = receiver noise figure in dB

I_E = emphasis improvement (4 dB with emphasis and 0 without)

C/N = predetection carrier-to-noise ratio in dB (N is the receiver front end thermal noise power in the same units as P_r

B_{IF} = receiver IF bandwidth in kHz = $2\ (\Delta F + f_m)$

ΔF = peak carrier deviation in kHz

PF = baseband signal peak factor (13.5 dB)

LF = rms noise load factor in dB

n = number of voice channels in baseband.

The value of P_r at which thermal noise threshold, TH, occurs is given by the equation:

$$P_r(TH) = -144 + 10 \log_{10}(B_{IF}) + F. \quad (4\text{-}10)$$

The value of P_r at which FM threshold occurs, FMTH, is:

$$P_r(FMTH) = K_T + P_r(TH) \quad (4\text{-}11)$$

where K_T = 10 without threshold extension and K_T = 3 with threshold extension.

The terms of the right-hand side of (4-6) with the exception of P_r may be calculated for a given set of equipment parameters. This then becomes a constant--a figure of merit--and as P_r is allowed to vary, the voice channel S/N varies in proportion. Using this information, a reciever thermal noise transfer characteristic or "quieting curve" may be constructed, where its slope is uniquely determined by either (4-6) or (4-7) for conditions above FM threshold.

Equipment Intermodulation Noise Calculation:

Equipment intermodulation noise, for the purpose of the system noise calculations,

is defined as the total noise from all sources produced as a result of the presence of a modulated signal in the system except feeder echo noise. Intermodulation noise is measured in a channel with all modulation removed from the channel being measured, and with all remaining channels loaded with actual traffic or with an equivalent amount of white noise over a specific bandwidth. The intermodulation noise power in the channel is then equal to the measured total noise with modulation present, less the measured thermal moise with no modulation present.

The values of noise power ratio (NPR) in the channel having the worst S/N must be obtained from either equipment performance specifications or carefully controlled tests. The specific loading conditions and received signal level (RSL) must be known for each NPR value. Of particular importance, is the NPR value corresponding to the optimum RSL for a particular EHF radio.

If information is not available, an NPR value of 55 dB obtainable using new, quality equipment is probably the highest value that can be assumed for the initial estimate. A pre-emphasis improvement of 4 dB in the worst channel is usually assumed included in this NPR value.

The noise power ratio can be converted to an equivalent noise channel signal-to-equipment intermodulation noise ratio, S/N_e, and additionally to equipment intermodulation noise, N_e:

$$S/N_e = NPR + 10 \log_{10}(B_b/b_c) - LF \quad dB \qquad (4\text{-}12)$$

$$N_e = 10^{(90 - S/N_e)/10} \qquad (4\text{-}13)$$

$$B_b = f_m - f_l \qquad (4\text{-}14)$$

where f_m = upper baseband frequency in kHz
f_l = lower baseband frequency in kHz
b_c = nominal voice channel bandwidth, 3.1 kHz
LF = rms load factor in dB (see equation 4-9).

In these noise calculations flat-weighted noise will be used for ease in handling. If the designer desires to use other noise weightings, appropriate factors may be included at the conclusion of the design procedure.

Feeder Intermodulation Noise Calculation:

If a transmission line many wavelengths long is mismatched at both the generator and load ends, its frequency-phase response is linear with a small sinusoidal ripple, and this leads to reflected waves in the line that cause distortion of an FM signal. This type of distortion is more conveniently considered as being caused by an echo signal generated in a mismatched line, which results in intermodulation distortion. Significant levels of this type of intermodulation noise are reached when the wave-

guide lengths exceed approximately 20 meters per individual antenna, or 30 meters total per hop (Dept. of Defense, 1977a, p. 4-284).

For EHF equipment it should seldom be necessary for waveguide lengths to exceed 1 meter. The resulting echo delay times of less than 6 nanoseconds should not contribute significant intermodulation noise for most bandwidths. Detailed information about waveguide type and velocities should therefore not be necessary except for wide bandwidths greater than approximately 50 MHz.

Feeder intermodulation noise, N_f, may be approximated given transmission line lengths, velocity of propagation in the lines, transmission system component voltage standing wave ratio's (VSWR) or return losses, transmission line losses, and directional losses. The calculations are performed separately for each end of a link; i.e., transmitter and receiver, and the results are summed to determine the total hop contribution.

To calculate N_f in the worst channel, the echo delay time, τ, is first calculated from the transmission line length, L, in meters and the velocity of propagation, V, in meters/second using:

$$\tau = 2L/V \quad \text{seconds} \tag{4-15}$$

where reasonable default values for V are 195,000,000 and 225,000,000 for elliptical and rectangular waveguide, respectively.

The echo delay time is then converted to radian delay using:

$$\theta_0 = 2\pi f_m \tau \times 10^3 \tag{4-16}$$

where f_m is the highest modulating frequency in the baseband. The echo power, r, relative to the signal power is given by the expression (Dept. of Defense, 1977a, pp. 4-286, 4-389):

$$r = RL_e + RL_a + 2A_{tl} \tag{4-17}$$

where r = number of dB that echo is down from the signal power

A_{tl} = transmission line loss in dB

RL_e = return loss (dB) at the interface between the transmission line and either the transmitter or receiver as applicable

RL_a = return loss (dB) at the interface between the transmission line and the antenna.

This model assumes that all discontinuities in the intermediate section of the transmission line between the transmitter or receiver and the antenna are negligible.

If parameters other than return loss are provided such as the VSWR or the voltage reflection coefficient, ρ, they can be converted to return loss, RL, using the

following expressions:

$$\rho = \frac{VSWR - 1}{VSWR + 1} \tag{4-18}$$

$$RL = 20 \log_{10}(1/\rho). \tag{4-19}$$

The power in the echo cannot totally be considered as distortion power, D, unless the echo delay is large. To obtain the value of the signal-to-distortion ratio, S/D, a parameter A must be determined:

$$A = \frac{\delta f}{f_m} \times 10^{\frac{LF}{20}} \tag{4-20}$$

or alternatively,

$$A = \frac{\delta f}{f_m} \times (n/10)^{1/2} \tag{4-21}$$

where the variables have been defined earlier in this section [see (4-6) and (4-7)].

The signal-to-distortion ratio minus the echo power, (S/D - r), can now be approximated (Hause and Wortendyke, 1979, p. 68) as the greater of F_1 and F_2 where:

$$F_1 = 7.17 - 8.23 \ln (A) + 40 \log (1/\theta_0) \tag{4-22}$$

$$F_2 = 9.412 - 54.84A + 113.2A^2 - 88.5A^3 + 31.52A^4 - 4.239A^5 \tag{4-23}$$

The calculations of echo attenuation (seperately for transmitter and reciver) outlined above can now be converted to voice channel noise. To do this, the total echo attenuation, r, is added to the value of (S/D - r) obtained from (4-22) and (4-23) above. This results in the signal-to-distortion ratio, S/D, which must be corrected for the ratio of baseband to voice channel bandwidth and for the RMS load factor. The voice channel signal to feeder echo noise ratio becomes:

$$S/N_f = S/D + 10 \log_{10} \frac{B_b}{b_c} - LF + I_E. \tag{4-24}$$

The conversion to flat-weighted noise is as follows:

$$N_f = 10^{(90 - S/N_f)/10} \quad pWO. \tag{4-25}$$

The foregoing feeder echo noise calculations are performed separately for each end of a hop and are summed to give a total link feeder echo noise contribution.

4.3.2 FM/FDM link availability

In this module the required performance level along with the single-receiver transfer characteristic and the cumulative distribution of RSL are used to compute the availability of the link, i.e., the fraction of time that the S/N of the worst channel is above the required minimum. An example of the output of this module is presented in Table 4-3.

Table 4-3. Example Output of the FM/FDM Link Performance Module

FM/FDM Link Performance
Lee Hill to Receiver Path

System Type		FM/FDM
Path Length	(km)	17.3

Long-term Distribution Parameters:

Long-term Median C/N	(dB)	40.9
Long-term Median RSL	(dBm)	-50.1
Equipment Noise S/N	(dB)	66.11
Xmtr Feeder Echo S/N	(dB)	80.64
Rcvr Feeder Echo S/N	(dB)	78.64
Thermal S/N - C/N	(dB)	20.08
Empasis Improvement	(dB)	4.0
P(FMTH) - P(TH)	(dB)	3.00

Link Performance

		Allowable	Calculated
Long-term Noise	(pW0)	55.40	1067.88
Short-term Noise	(dB)	500000.0	500000.0
Availability		0.999980	0.996494
Fade Margin	(dB)	30.0	28.0

Defense communication system (DCS) noise requirements:

On the basis of a hypothetical reference circuit, MIL-STD-188-300 (Dept. of Defense, 1971) in paragraph 4.3.3.1.2 allocates a maximum of 3.33 pWp0/km median noise level in the noisiest voice channel due to radio equipment and propagation. This value translates to approximately 3.2 pW0/km (flat weighting). In order to provide a design objective this value was selected as a standard of analog link quality. The 3.2 pW0/km value seems to be consistent with CCIR (1978) and industry standards for high performance links (Brodhage and Hormuth, 1968, p. 22). Most of this noise allocation is assigned to equipment noise since thermal noise is a small component at the median signal level. It should not be cause for alarm if an individual link's median noise level does not fall within this noise allowance since it is the summation of the median noise values for all the links on a route that is important.

For short-term performance considerations, the maximum allowable flat weighted noise is 500,000 pW0 in the worst channel, MIL-STD-188-313, sec. 4.1.2.1.1.2, Dept. of Defense (1973). This value corresponds to a value of S/N in the worst channel of 33 dB. The S/N ratio is allowed to fall below 33 dB for no more than 10 minutes per year (approximately 2 min during the worst month, Dept. of Defense, 1977a, p. 4-261) which is equivalent to an average availabitity of 0.99998 of the year. The value of 0.99998 is used in ETSEM for all time periods.

FM/FDM performance and availability

The allowable long-term noise level in the worst channel is calculated using:

$$N = 3.2L \quad \text{pW0} \tag{4-26}$$

where L is the path length. The predicted long-term noise is calculated using:

$$N = N_t + N_e + N_f \quad \text{pW0} \tag{4-27}$$

where the long-term thermal noise is found from (4-6) using the long-term median RSL and N_e and N_f are found from (4-13) and (4-25).

The allowable short-term noise and availability are fixed as 500,000 pW0 and 0.99998 in accordance with the design objectives presented above. The predicted availability is found in the following manner using the combined cumulative distribution of RSL discussed in section 3.5:

1. Using (4-27) and (4-6) the RSL corresponding to 500,000 pW0 of noise in the worst channel is found.
2. This RSL is used to compute the availability as follows:
   a. If this RSL is greater than the greatest RSL in the combined distribution then the availability is less

than the lowest availability of the distribution (about 0.9) and a message to this effect is included in the output.

b. If this RSL is less than the lowest RSL in the combined distribution then the availability is greater than 0.999999. In this case an availability of 0.999999 is taken and a new worst channel short-term noise level less than 500,000 pW0 is computed for the RSL from the distribution corresponding to an availability of 0.999999.

c. If neither condition in a. or b. is met, then the RSL is used to interpolate the availability from the combined distribution. Linear interpolation is applied to the common logarithm of the percentage of time the signal is below level.

The allowable fade margin is fixed at 30 dB as a design objective. The predicted fade margin is calculated as the long-term median RSL minus the RSL corresponding to the short-term noise level.

4.4 Digital Modulation Performance Module

The purpose of this module is to predict the availability of digital links; i.e., the fraction of time that the bit error rate (BER) is less than some required performance standard. This is performed by assuming a standard shape for digital receiver transfer characteristics and adjusting the level according to equipment specifications. The RSL required to meet the performance specifications is then found from the specific digital receiver transfer characteristic. This RSL is then used to find the availability from the combined distribution of RSL discussed in section 3.5. An example of the output of this module is presented in Table 4-4.

4.4.1 Defense communication system digital link requirements:

MIL-STD-188-322 (Dept. of Defense, 1976) states that for LOS digital microwave systems: "It is a design objective to have a 30 dB minimum fade margin on all paths. All radio links are required to have a minimum annual path availability of 0.99995 for maintaining a bit error rate of 5×10^{-9} for operation below 10 GHz. All radio links are also required to have a minimum annual path availability of 0.99998 for maintaining a bit error rate of 1×10^{-2}."

In ETSEM these design objectives are extended to 100 GHz. Only the short-term requirement of a path availability of 0.99995 of BERs less than 5×10^{-9} has been included in ETSEM. Long-term or median path performance (for error rates substantially

Table 4-4. Example Output of the Digital Link Performance Module

Digital Link Performance
Lee Hill to Receiver Path

Modulation Type		fm
Data Transmission Rate	(Mb/s)	12.6
Frequency	(GHz)	42.0
Path Length	(km)	17.3
Long-term Median RSL	(dBm)	-50.1

Manufacturer's Equipment Specifications

Reference RSL	(dBm)	-71.0
Reference BER		1.00e-07

Link Performance

		Allowable	Calculated
BER		5.00e-09	5.00e-09
Availability		0.999950	0.994176
Fade Margin	(dB)	30.0	20.0

Allowable availability is not satisfied.

Note: These values cover propagation effects, not equipment outages.

less than 5×10^{-9}) are not meaningful since such low error rates are generally a function of equipment performance, not path performance.

4.4.2 Digital receiver transfer characteristic

Although the BER threshold will vary for various types of digital receivers, the shape of the transfer characteristic will generally remain the same in the presence of Gaussian noise (Bell Telephone Labs., 1970, p. 629). The equation for the receiver transfer characteristic is:

$$BER = \frac{1}{2} \operatorname{erfc}(k_0 \times 10^{P_r/20}) \qquad (4\text{-}28)$$

where the constant, k_0, is equipment dependent. The error function compliment, erfc, is found from

$$\operatorname{erfc}(x) = 1 - \operatorname{erf}(x) \qquad (4\text{-}29)$$

where the error function is evaluated using (3-26) through (3-32).

The constant, k_0, is found from equipment specifications that give the BER at a reference RSL, P_r. ETSEM does this by iteratively adjusting k_0 until (4-28) gives the reference BER for the reference RSL.

4.4.3 Digital link availability

The allowable short-term BER and availability are fixed in ETSEM as 5×10^{-9} and 0.99995 in accordance with the design objectives presented above. The predicted availability is found in the following manner using the combined cumulative distribution of RSL discussed insection 3.5:

1. The constant, k_0, is first found as discussed in section 4.4.2.
2. The RSL corresponding to the allowable short-term BER is then found by iteratively solving (4-28) for P_r.
3. This RSL is then used to compute the availability as follows:
   a. If this RSL is greater than the greatest RSL in the combined distribution, then the availability is less than the lowest availability of the distribution (about 0.9) and a message to this effect is included in the output.
   b. If this RSL is less than the lowest RSL in the combined distribution, then the availability is greater than 0.999999. In this case an availability of 0.999999 is taken and a new BER less than the allowable short-term is computed using (4-28) for the RSL from the distribution corresponding to an availability of 0.999999.
   c. If neither condition in a. or b. above is met, then the RSL is used to interpolate the availability from the combined

distribution. Linear interpolation is applied to the common logarithm of the percentage of time the signal is below level.

The allowable fade margin is fixed at 30 dB as a design objective. The predicted fade margin is calculated as the long-term median RSL minus the RSL corresponding to to the short-term allowable BER as found in step 2 above.

5. SUMMARY

ETSEM, EHF Telecommunication System Engineering Model, has been developed to aid in the engineering of line-of-sight telecommunication systems from 10 to 100 GHz. The model has been implemented on an HP 9825 desktop computer and uses equipment specifications and models of propagation effects to predict the performance (availability) of the link.

The cumulative distribution of the bit error rate for digital links and the cumulative distribution of the worst channel signal-to-noise ratio for FM-FDM links are predicted. These measures of performance are predicted for any interval of months out of the year.

The model includes several innovations and enhancements over previously existing models. One of these is the ability to predict monthly statistics of performance instead of just annual. This required the modification of the Rice-Holmberg model. Another feature is a new model of attenuation due to atmospheric oxygen in the form of an expansion in pressure and temperature.

ETSEM represents a state-of-the-art attempt to predict the performance of telecommunication links above 10 GHz. As such, the models are substantially untested. Only actual link performance data will verify the accuracy of the models and lead to improvements in ETSEM.

There are several weaknesses in ETSEM as the result of the nonavailability of EHF propagation models and data. There are also, of course, several improvements that could be made to the model that are apparent at this time. These are discussed in the next section of this report.

6. RECOMMENDATIONS

Because rain is the greatest threat to EHF link performance, improvements in rain attenuation models are the most critical. The most important improvement would be the inclusion of specific attenuation parameters (drop-size dependent) that have been experimentally verified for EHF frequencies. Such parameters do not exist at this time and extensive experimental data would be required to develop them.

The rain attenuation model could also be improved by the development of a

formulation for the thunderstorm ratio based on measured monthly data. Such a formulation would give the thunderstorm ratio as a function of commonly available monthly rain statistics.

A third improvement in the rain attenuation predictions could be made, at least for locations in the United States, by including more U. S. stations in the meteorological data base. This would reduce the error resulting from the interpolation of the rain model parameters.

Another obvious need for the model is the development of a multipath fading model that predicts not the worst month fading statistics but the fading statistics of each of the months of the year. One possible approach would be to scale the worst month predictions to the other months based on monthly meteorological parameters. Such a model would have to be based on the analysis of measured data.

A variety of other improvements are possible, such as the addition of meteorological data bases for other regions of the world, the addition of models for other types of modulation or telecommunication equipment, and enhanced output from the program.

The experimental testing of the model is desirable. By illustrating ETSEM's strengths and weaknesses, such tests would point to what efforts should be made to improve the model and indicate the reliability of the predictions. By selecting the location of these test paths, the importance of propagation effects not included in ETSEM such as attenuation by clouds, fog, and dust could be evaluated.

7. ACKNOWLEDGMENTS

The author would like to thank Dr. Hans Liebe for his helpful guidance on the development of a more computationally efficient algorithm for specific oxygen absorption. The author would also like to thank Greg Hand who did the computer programming to develop the new oxygen absorption algorithm and Dan Cronin who did most of the programming of ETSEM. Thanks is also due to Larry Hause for his consistent help in explaining the ADSEM and WORLD programs, which are in some sense the parents of ETSEM.

8. REFERENCES

Abramowitz, M. and I. A. Stegun (1964), Handbook of Mathematical Functions, National Bureau of Standards.

Allen, K. C. (1983), Attenuation of Millimeter Waves on Earth-Space Paths by Rain Clouds, NTIA Report 83-132 (NTIS Access. No. PB84-115120).

Allen, K. C., H. J. Liebe, and C. M. Rush (1983), Estimates of Millimeter Wave Attenuation for 18 United States Cities, NTIA Report 83-119 (NTIS Access. No. PB83-240630).

Allen, K. C., R. H. Ott, E. J. Viollette, and R. H. Espeland (1982), Height-Gain Study for 23 km Links at 9.6, 11.4, and 28.8 GHz, IEEE Trans. Ant. Prop. AP-30, No. 4, pp. 734-740.

Barnett, W. T. (1972), Multipath Propagation at 4, 6, and 11 GHz, Bell System Technical Journal, Vol. 56, No. 2, pp. 321-361.

Bean, B. R. and B. A. Cahoon (1957), A Note on the Climatic Variation of Absolute Humidity, Bull. American Met. Soc., Vol. 38, No. 7, pp. 395-398.

Bell Telephone Laboratories (1970), Transmission Systems for Communications (Western Electric Company, Inc., Winston-Salem, N. C.).

Bryson, R. A. and F. K. Hare, editors, Climates of North America, World Survey of Climatology, Vol. 11, Elsevier Scientific Publishing Company, New York.

Brodhage, H. and W. Hormuth (1968), 7th Ed., Planning and Engineering of Radio Relay Links, (Siemens Aktiengsellschaft, Munich, Germany)

CCIR (1978), Noise in the radio portion of circuits to be established over real radio-relay links for FDM telephony, Vol 9, Rec. 395-2, XIV Plenary Assembly, KYOTO, Japan.

CCIR (1982), Pre-emphasis characteristic for frequency modulation radio-relay systems for telephony using frequency-division multiplex, Vol. 9, Rec. 275-3, XV Plenary Assembly, Geneva, Switzerland.

Crane, R. K. (1980), Prediction of attenuation by rain, IEEE Trans. Comm. COM-28, No. 9, pp. 1717-1733.

Crombie, D. D. (1983), Prediction of Multipath Fading on Terrestrial Microwave Links at Frequencies of 11 GHz and Greater, AGARD/NATO Conference Proc. No. 346.

Department of the Army (1967), Grid and Grid References, Technical Bulletin No. TM5-241-1, Headquarters Department of the Army, Washington, D.C.

Department of Defense (1971), Standards for Long Haul Communications - System Design/ Standards Applicable to the Defense Communications System, MIL-STD-188-300.

Department of Defense (1973), Subsystem Design and Engineering Standards and Equipment Technical Design Standards for Long-haul Communications Transversing Microwave LOS Radio and Tropospheric Scatter Radio, MIL-STD-188-313.

Department of Defense (1976), Subsystem Design/Engineering and Equipment Technical Design Standards for Long-Haul Line-of-sight (LOS) Digital Microwave Radio Transmission, MIL-STD-188-322.

Department of Defense (1977a), Design Handbook for Line-of-sight Microwave Communication System, MIL-HDBK-416.

Department of Defense (1977b), Facility Design for Tropospheric Scatter, MIL-HDBK-417.

Dutton, E. J. (1984), Microwave Terrestrial Link Rain Attenuation Prediction Parameter Analysis, NTIA Report 84-148 (NTIS Access. No. PB84-207984).

Dutton, E. J., C. E. Lewis, F. K. Steele (1983), Climatological Coefficients for Rain Attenuation at Millimeter Wavelengths, NTIA Report 83-129 (NTIS Access. No. PB84-104272).

Espeland, R. H., E. J. Violette, and K. C. Allen (1984), Atmospheric Channel Perfromance Measurements at 10 to 100 GHz.

Hause, L. G. and D. R. Wortendyke (1979), Automated Digital System Engineering Model, NTIA Report 79-18 (NTIS Access. No. PB294960).

Joss, J., J. C. Thams, and A. Waldvogel (1968), The Variation of Rain Drop Size Distribution at Locarno, Proc. Int. Cong. Cl Physics, pp. 369-373.

Liebe, H. J. (1983), An Atmospheric Millimeter Wave Propagation Model, NTIA Report 83-137 (NTIS Access. No. PB84-143494).

List, R. J. (1951), Smithsonian Meteorological Tables, 6th Ed., (Smithsonian Institution, Washington, D.C.).

Olsen, R. L., D. V. Rogers, and D. B. Hodge (1978), The aRb Relation in the Calculation of Rain Attenuation, IEEE Trans. Ant. Prop. AP-26, No. 2, pp. 318-329.

Rice, P. L. and N. R. Holmberg (1973), Cumulative Time Statistics of Surface-Point Rainfall Rates, IEEE Trans. Comm., Vol. COM-21, No. 10, pp. 1131-1136.

Schiavone, J. A. (1981), Prediction of Positive Refractivity Gradients for Line-of-Sight Microwave Radio Paths, Bell Sys. Tech. J. 60, No. 6, pp. 803-822.

Shanmugan, K. S., V. S. Frost, J. C. Hotzman, E. M. Friedman, and M. McKinley, "EHF Channel Modeling and Simulation," RADC Tech. Report 85-100.

Thomas, P. D. (1970), Spheroidal Geodesics, Reference Systems, and Local Geometry, (U.S. Naval Oceanographic Office, Washington, D.C. 20390).

Vigants, A. (1981), Microwave Radio Obstruction Fading, Bell Sys. Tech. J., 60, No. 6, pp. 785-801.

Webster, Alan R. (1983), Angles of Arrival and Delay Times of Terrestrial Line-of-Sight Microwave Links, IEEE Trans. Ant. Prop. AP-31, No. 1, pp. 12-17.

Wallen, C. C., editor (1970), Climates of Northern and Western Europe, World Survey of Climatology, Vol. 5, Elsevier Scientific Publishing Company, New York.

Wallen, C. C., editor (1977), Climates of Central and Southern Europe, World Survey of Climatology, Vol. 6, Elsevier Scientific Publishing Company, New York.

APPENDIX A: ANTENNA DECOUPLING AND k FACTORS

A simple approach to the problem of antenna decoupling is to first assume that the variations in angle of arrival can be attributed to changes in the k factor (effective earth radius factor). This amounts to assuming that variation in angle of arrival due to atmospheric layers with short height intervals are dominated by the variations due to large-scale changes in the gradient of the refractive index from the ground up through the greatest height of interest for the path. With this assumption and the assumption that the antennas are pointed directly at each other under condition for which $k = k_0$ (an arbitrary reference condition), the distribution of the angle of arrival about the boresight can be found from the distribution of the k factor.

Using (2-4) it can be seen that the deviation of the angle of arrival from the center of the beam becomes

$$\beta = \tan^{-1} (d/D - D/12750k) - \tan^{-1} (d/D - D/12750k_0) \qquad (A\text{-}1)$$

where d is the difference in antenna heights (receiver and transmitter) and D is the path length, both in km. Solving (A-1) for k gives

$$k = \frac{D}{12750(d/D - \tan [\beta + \arctan (d/D - D/12750k_0)]} \qquad (A\text{-}2)$$

from which it is possible to find the k factor which would result in the deviation β of the angle of arrival from the center of the beam.

In general, because of the probability distribution of surface refractivity gradients, it is small k factors that will cause the most antenna decoupling. As a rough approximation, the k factor will be less than 0.1 only about 0.1 percent of the year in most locations. In order to estimate the threat of antenna decoupling, the antenna beamwidths can be assumed to be equal and the difference in antenna heights can be assumed to be zero. In this case a deviation of the angle of arrival from the center of the beam equal to the 3 dB beamwidth would result in a fade of 6 dB (3 dB at each antenna). If $k_0 = 4/3$, then (A-1) can be used to find the 3 dB beamwidth for which antenna decoupling fading has the potential of becoming significant. That is, roughly, the antenna decoupling fading would be expected to exceed 6 dB for 0.1 percent of the year (an availability of 0.999) for a beamwidth of 0.4° for a 10 km path, 1° for a 25 km path, and 2° for a 50 km path.

Thus if the beamwidths approach 0.04° per kilometer of path length, some caution should be exercised by consulting Samson (1975) or Schiavone (1981). This is especially true if the path is near a large body of water.

REFERENCES

Samson, C. A. (1975), Refractivity gradients in the northern hemisphere, OT Report 75-59 (NTIS Access. No. COM75-10776/AS).

Schiavone, J. A. (1981), Prediction of Positive Refractivity Gradients for Line-of-Sight Microwave Radio Paths, Bell Sys. Tech. J. 60, No. 6, pp. 803-822.

APPENDIX B: COMPUTATIONALLY FAST OXYGEN ABSORPTION MODEL

The model of Liebe (1983), while one of the most accurate, requires too much computation time to be used on a desk-top computer for ETSEM. The computation of the line-by-line contributions to the oxygen absorption are responsible for much of the time needed to predict the attenuation in the 10 to 100 GHz range. Therefore a number of approaches were used to approximate the oxygen attenuation predicted by Liebe's model by faster algorithms.

The goal was to find a fast algorithm that only differed at most by 10 percent from Liebe's for pressures from sea level to 4,570 m (15,000 ft) of altitude and temperatures from 240 to 320 Kelvin. The model would then be satisfactory for nearly all ground-to-ground, line-of-sight paths.

One approach was to attempt to lower the number of resonant lines by eliminating weaker ones. A sufficient decrease in computation time could not be achieved with this approach.

Another approach was to approximate the absorption band near 60 GHz with the summation of a few lines. Even for just one temperature and pressure, the 10 percent limit on error could not be achieved with four or less lines using four different line shapes. The piecewise fitting together over the 10 to 100 GHz frequency range of several lines also did not appear promising when tried.

The only approach that met the requirements was the expansion of the attenuation in terms of pressure and temperature. Different expansions were tried at several frequencies and the residues as functions of temperature and pressure were studied. This led to the selection of

$$A = a\,\theta^{\beta_1}\,P^{\beta_2}\exp(\beta_3\theta^2 + \beta_4\theta^2 P) \qquad \text{(B-1)}$$

as the optimum expansion meeting the accuracy requirements but containing a minimum of terms. In (B-1), specific attenuation, dB/km, is denoted by A, P denotes pressure, and $\theta = 300/T$ denotes the relative inverse pressure where T is in Kelvin.

The parameters, a, β_1, β_2, β_3, and β_4, were found by doing a least-squares fit after taking the logarithms of both sides of (B-1). The least-squares fit was done for a selection of frequencies and the resulting parameters are given in Table (B-1). If for any frequency between 10 to 100 GHz, parameters are interpolated from the table (the interpolation should be done on log(a), not a and (B-1) is used, the computed specific oxygen absorption will differ from that of the Liebe model by less than 6.5 percent over the restricted range of temperatures and pressures given above.

REFERENCES

Liebe, H. J. (1983), An Atmospheric Millimeter Wave Propagtion Model, NTIA Report 83-183 (NTIS Access. No. PB84-143494).

TABLE B-1

Parameters for the Oxygen Absorption Model

Frequency (GHz)	β_1	β_2	β_3	β_4	log(a)
1.0	1.95486	1.61977	0.585255	0.0498012	-12.4725
2.0	1.95420	1.42601	0.667142	0.0505578	-11.1674
3.0	1.94434	1.99489	0.416288	0.0613680	-10.1134
4.0	1.96334	1.17008	0.783619	0.0402274	-9.88077
5.0	1.97500	1.58767	0.615410	0.0279332	-9.24827
6.0	1.95481	1.59874	0.592513	0.0499846	-8.87709
7.0	1.96107	1.78695	0.517203	0.0431519	-8.47907
8.0	1.97249	1.38130	0.699036	0.0306508	-8.37309
9.0	1.96344	1.68724	0.560245	0.0405410	-7.99898
10.0	1.97763	1.47874	0.660462	0.0250488	-7.86214
11.0	1.95329	1.59252	0.589813	0.0517457	-7.61604
12.0	1.94521	1.61049	0.574179	0.0604609	-7.42212
13.0	1.96023	1.52270	0.623438	0.0439955	-7.28016
14.0	1.95185	1.72352	0.529248	0.0533365	-7.03135
15.0	1.96402	1.72906	0.536381	0.0398855	-6.86982
16.0	1.97544	1.50862	0.638688	0.0274371	-6.81220
17.0	1.95035	1.81141	0.486253	0.0550011	-6.54655
18.0	1.97763	1.56945	0.611240	0.0252578	-6.50590
19.0	1.94195	1.66799	0.536601	0.0640628	-6.33999
20.0	1.97721	1.47771	0.646332	0.0256691	-6.28394
21.0	1.96360	1.63077	0.567286	0.0406799	-6.09667
22.0	1.95906	1.68327	0.538818	0.0456336	-5.95271
23.0	1.94487	1.75428	0.493892	0.0612693	-5.80556
24.0	1.97558	1.66308	0.557251	0.0276769	-5.71870
25.0	1.97589	1.75204	0.517187	0.0273601	-5.56374
26.0	1.96094	1.79046	0.484984	0.0438731	-5.43501
27.0	1.97230	1.57630	0.583410	0.0313882	-5.40856
28.0	1.96361	1.70461	0.518263	0.0410052	-5.24123
29.0	1.98315	1.65915	0.551399	0.0199747	-5.14129
30.0	1.96369	2.02511	0.375443	0.0413185	-4.87503
31.0	1.97233	1.87259	0.444422	0.0320019	-4.82253
32.0	1.97403	1.97619	0.398195	0.0302870	-4.66160
33.0	1.97815	1.90335	0.428849	0.0260427	-4.57406
34.0	1.98604	1.89165	0.436595	0.0176214	-4.45790
35.0	1.98633	1.86576	0.443494	0.0175648	-4.34766
36.0	1.98436	2.03378	0.365666	0.0199792	-4.15287
37.0	1.99040	1.84685	0.445584	0.0136080	-4.10461
38.0	1.98699	2.02314	0.362225	0.0177196	-3.90030
39.0	1.98997	1.83701	0.438255	0.0148443	-3.84496
40.0	1.98667	2.00631	0.357039	0.0189902	-3.63493
41.0	1.98661	2.15159	0.288226	0.0197038	-3.42880
42.0	1.98981	2.04864	0.327180	0.0168998	-3.32121
43.0	1.96726	2.27381	0.203083	0.0423335	-3.07211
44.0	1.98290	2.01225	0.318149	0.0262591	-3.01202
45.0	1.98834	2.18710	0.236819	0.0217002	-2.75687

TABLE B-1 (continued)

Parameters for the Oxygen Absorption Model

Frequency (GHz)	β_1	β_2	β_3	β_4	log(a)
45.5	1.99354	2.07330	0.283154	0.0167537	-2.70937
46.0	1.98749	2.12228	0.249730	0.0241787	-2.59118
46.5	1.98841	2.05270	0.271882	0.0241100	-2.51720
47.0	1.99238	2.07954	0.254467	0.0209324	-2.39604
47.5	1.98292	2.02500	0.258664	0.0323832	-2.30656
48.0	1.98836	2.02263	0.251536	0.0278110	-2.18352
48.5	1.98259	2.03267	0.226404	0.0355120	-2.04799
49.0	1.98281	1.99747	0.221107	0.0362504	-1.91647
49.5	1.96348	1.74832	0.282919	0.0562961	-1.86067
50.0	1.94220	1.53381	0.318982	0.0757375	-1.76405
50.5	1.89450	1.20989	0.366943	0.117463	-1.68332
51.0	1.81732	0.787649	0.418539	0.179395	-1.60264
51.5	1.69918	0.297965	0.455469	0.266921	-1.50430
52.0	1.54438	-0.187705	0.462673	0.369556	-1.35963
52.5	1.36251	-0.442927	0.370336	0.471964	-1.08387
53.0	1.19512	-0.483840	0.239733	0.535249	-0.705629
53.5	1.06736	-0.302879	0.0990923	0.540135	-0.243124
54.0	0.982303	0.0435821	-0.0263568	0.492889	0.260572
54.5	0.942847	0.355419	-0.0598411	0.402182	0.707710
55.0	0.925115	0.782852	-0.0979265	0.293603	1.15904
55.5	0.915716	1.05951	-0.0502190	0.180387	1.50105
56.0	0.870940	1.42820	-0.0750578	0.113704	1.83154
56.1	0.859827	1.51084	-0.0894423	0.108090	1.89407
56.2	0.857335	1.46687	-0.0436644	0.0941686	1.90294
56.3	0.852496	1.56757	-0.0635772	0.0857917	1.97017
56.4	0.852032	1.63636	-0.0690505	0.0775190	2.02104
56.5	0.872313	1.71795	-0.0648099	0.0514307	2.07862
56.6	0.891847	1.66098	-0.00393518	0.0287276	2.07414
56.7	0.908700	1.72631	0.00178448	0.00929175	2.11984
56.8	0.918283	1.85152	-0.0246470	-0.00268600	2.18847
56.9	0.923842	1.82837	0.00803159	-0.00996514	2.19141
57.0	0.929350	1.88182	0.00695311	-0.0153091	2.22470
57.1	0.945999	1.88723	0.0349656	-0.0309695	2.23798
57.2	0.974042	1.97991	0.0354314	-0.0588825	2.29007
57.3	0.971802	2.06896	0.0118835	-0.0559591	2.33344
57.4	0.990907	2.02538	0.0645214	-0.0794549	2.32624
57.5	0.983120	2.05487	0.0633886	-0.0757642	2.34405
57.6	0.991531	2.13479	0.0545946	-0.0896940	2.38660
57.7	0.987883	2.11646	0.0764949	-0.0897597	2.38328
57.8	0.996262	2.22046	0.0563633	-0.102854	2.43455
57.9	0.993897	2.32193	0.0286151	-0.106432	2.48277

TABLE B-1 (continued)

Parameters for the Oxygen Absorption Model

Frequency (GHz)	β_1	β_2	β_3	β_4	log(a)
58.0	0.999447	2.27136	0.0733340	-0.122051	2.46978
58.1	0.966830	2.17804	0.103730	-0.0990851	2.43073
58.2	0.924242	2.39375	-0.00690383	-0.0651769	2.52094
58.3	0.918436	2.28927	0.0482810	-0.0678975	2.48146
58.4	0.921950	2.40552	0.0137269	-0.0744359	2.53501
58.5	0.947951	2.27608	0.0996520	-0.0993662	2.48572
58.6	0.962677	2.40925	0.0609408	-0.107472	2.54340
58.7	1.00177	2.49830	0.0610791	-0.141396	2.58774
58.8	1.02084	2.45038	0.102220	-0.155537	2.57007
58.9	1.02811	2.59155	0.0533529	-0.160078	2.63224
59.0	1.01570	2.43796	0.113771	-0.146434	2.56570
59.1	1.00367	2.67617	0.00747481	-0.134317	2.66750
59.2	1.01140	2.44810	0.116210	-0.143725	2.57541
59.3	1.02231	2.54043	0.0899128	-0.155226	2.62061
59.4	1.01641	2.61444	0.0556916	-0.147584	2.65395
59.5	1.01806	2.65688	0.0405179	-0.147827	2.67607
59.6	1.03140	2.63436	0.0626836	-0.161576	2.67441
59.7	1.03926	2.61196	0.0801400	-0.171235	2.67309
59.8	1.04696	2.65807	0.0688510	-0.183636	2.70314
59.9	1.03073	2.63383	0.0676411	-0.173841	2.70003
60.0	1.00471	2.57567	0.0733128	-0.157127	2.68241
60.1	0.976614	2.45600	0.103253	-0.139922	2.63935
60.2	0.932906	2.52231	0.0389860	-0.104589	2.67141
60.3	0.919576	2.41037	0.0737578	-0.0976653	2.63242
60.4	0.907440	2.50473	0.0173632	-0.0846362	2.67771
60.5	0.927025	2.34846	0.0905804	-0.0984212	2.61963
60.6	0.961421	2.48287	0.0492974	-0.122469	2.68597
60.7	0.991865	2.32049	0.129164	-0.140422	2.62379
60.8	1.01631	2.33759	0.127275	-0.153341	2.63768
60.9	1.03017	2.48827	0.0606812	-0.158866	2.70810
61.0	1.03413	2.48214	0.0536115	-0.157692	2.71134
61.1	1.02666	2.29504	0.114268	-0.146581	2.63599
61.2	1.03614	2.33173	0.0947994	-0.155154	2.66044
61.3	1.03587	2.29735	0.0971827	-0.154007	2.65249
61.4	1.04318	2.34420	0.0723399	-0.163424	2.68191
61.5	1.02822	2.38013	0.0343434	-0.152441	2.70280
61.6	1.01083	2.36335	0.0181777	-0.142724	2.70212
61.7	0.982231	2.20796	0.0523981	-0.123608	2.64013
61.8	0.959546	2.18968	0.0333936	-0.111327	2.63720
61.9	0.945431	2.17145	0.0213196	-0.107836	2.63481

TABLE B-1 (continued)

Parameters for the Oxygen Absorption Model

Frequency (GHz)	β_1	β_2	β_3	β_4	log(a)
62.0	0.918870	2.20500	-0.0240673	-0.0904391	2.64989
62.1	0.889055	2.03067	0.0156229	-0.0695574	2.57426
62.2	0.861393	2.03167	-0.0182127	-0.0507204	2.57231
62.3	0.820922	2.01417	-0.0574446	-0.0152189	2.55653
62.4	0.808747	1.96250	-0.0611401	-0.00483903	2.52852
62.5	0.800804	1.85970	-0.0442667	0.00890101	2.47421
62.6	0.81415	1.87559	-0.0640241	0.0067971	2.47046
62.7	0.822885	1.89708	-0.0940984	0.0151393	2.46409
62.8	0.845183	1.82527	-0.0752679	0.0116412	2.41846
62.9	0.854839	1.81111	-0.0943742	0.0244546	2.39200
63.0	0.878061	1.78175	-0.0972635	0.0249596	2.35976
63.5	0.930990	1.42865	-0.0875068	0.0982009	2.07438
64.0	0.937369	1.16460	-0.150265	0.205607	1.78983
64.5	0.935917	0.771836	-0.155374	0.318696	1.41269
65.0	0.956507	0.478773	-0.169455	0.417157	1.03578
65.5	1.00160	0.134719	-0.116021	0.496960	0.593757
66.0	1.09052	-0.133790	-0.0209506	0.535551	0.144537
66.5	1.21244	-0.222678	0.0734510	0.530814	-0.255899
67.0	1.37186	-0.0840023	0.151726	0.471443	-0.570263
67.5	1.54355	0.279256	0.183287	0.375933	-0.777264
68.0	1.69626	0.845835	0.132957	0.273969	-0.865682
68.5	1.82238	1.40113	0.0686404	0.177887	-0.915275
69.0	1.89950	1.97478	-0.0534956	0.116895	-0.914146
69.5	1.94685	2.41404	-0.156488	0.0763318	-0.928938
70.0	1.97327	2.73188	-0.237677	0.0519941	-0.963161
70.5	1.98795	3.04000	-0.334414	0.0373769	-0.977004
71.0	1.99103	3.16017	-0.368638	0.0330769	-1.05233
71.5	2.00055	3.27523	-0.399954	0.0211954	-1.11374
72.0	1.99553	3.31917	-0.416689	0.0251604	-1.19869
72.5	1.99351	3.55661	-0.515295	0.0260931	-1.19241
73.0	2.00472	3.53986	-0.495671	0.0126155	-1.28469
73.5	2.00287	3.66459	-0.548798	0.0136025	-1.31427
74.0	2.00237	3.74998	-0.585004	0.0132574	-1.35537
74.5	1.99885	3.68277	-0.559369	0.0160753	-1.45815
75.0	2.00784	3.82885	-0.614372	0.00549678	-1.46309
76.0	1.99550	4.06392	-0.727943	0.0176507	-1.49481
77.0	2.00465	4.05904	-0.721964	0.00637660	-1.61250
78.0	2.00256	4.26725	-0.817792	0.00769325	-1.63248
79.0	1.99607	4.44509	-0.905370	0.0139455	-1.65845
80.0	2.00321	4.41686	-0.894077	0.00533721	-1.76195
81.0	2.00652	4.64275	-0.995069	0.00111285	-1.75171
82.0	1.99645	4.87951	-1.11292	0.0116249	-1.73461
83.0	2.01400	4.93565	-1.13029	-0.00803782	-1.78292
84.0	2.01222	5.17302	-1.24206	-0.00660202	-1.75417

TABLE B-1 (continued)

Parameters for the Oxygen Absorption Model

Frequency (GHz)	β_1	β_2	β_3	β_4	log(a)
85.0	2.00515	5.28100	-1.30385	0.000676639	-1.77781
86.0	2.01625	5.48066	-1.38937	-0.0116559	-1.75429
87.0	2.01143	5.52630	-1.42342	-0.00681639	-1.79692
88.0	2.01691	5.60959	-1.46515	-0.0130106	-1.81774
89.0	2.00634	5.85770	-1.59133	-0.00172360	-1.76925
90.0	2.02222	5.73353	-1.53628	-0.0193594	-1.87054
91.0	2.00462	6.16059	-1.74542	-0.000372294	-1.74227
92.0	2.00838	6.33771	-1.82999	-0.00468204	-1.71303
93.0	2.01673	6.63615	-1.96272	-0.0138196	-1.62868
94.0	2.01691	6.62899	-1.97277	-0.0142589	-1.67445
95.0	2.03091	6.71337	-2.01008	-0.0297829	-1.67588
96.0	2.02189	6.95160	-2.13337	-0.0201087	-1.61535
97.0	2.02746	7.19390	-2.24632	-0.0261827	-1.54759
98.0	2.04383	7.34074	-2.30946	-0.0442275	-1.51623
99.0	2.00921	7.57121	-2.45297	-0.00663674	-1.45994
100.0	2.02274	7.90961	-2.60121	-0.0213829	-1.34416

APPENDIX C: ABSOLUTE HUMIDITY VARIABILITY

Bean and Cahoon (1957) modeled the cumulative distribution of absolute humidity in g/m^3 by giving the level of absolute humidity exceeded for selected percentages of the month in terms of the mean absolute humidity of the month. In particular, the level of absolute humidity, ρ, exceeded 1 percent of the month was given as

$$\rho = 0.99\bar{\rho} + 4.83 \qquad \text{(C-1)}$$

where $\bar{\rho}$ is the monthly mean absolute humidity. In a similar way the absolute humidities exceeded 5 and 10 percent of the month are given respectively by

$$\rho = 1.01\bar{\rho} + 3.36 \qquad \text{(C-2)}$$

and

$$\rho = 1.03\bar{\rho} + 2.63. \qquad \text{(C-3)}$$

For ETSEM a distribution of the absolute humidity during a month is needed which gives the level exceeded for whatever percentage of time is of interest. Several distributions were compared with the above equations, including the Rayleigh and Chi square distributions, but the Gaussian distribution agreed most closely. The data presented by Bean and Cahoon also indicated that the absolute humidity was approximately Gaussian distributed within an average month.

Thus ρ can be modeled as Gaussian distributed and the fraction of time, P, that the absolute humidity, ρ, is exceeded is given by

$$P(\rho) = [\, 1 - \text{erf}\, (\frac{\rho - \bar{\rho}}{\sigma\sqrt{2}})]/2 \qquad \text{(C-4)}$$

where erf symbolizes the error function and σ is the standard deviation of the absolute humidity for the selected month. All that is needed is an expression for the standard deviation.

By fixing P at 0.1, 0.05, or 0.01 a constant corresponding to the argument of the erf in (C-4) can be found as

$$c(P) = \frac{\rho - \bar{\rho}}{\sigma\sqrt{2}} \qquad \text{(C-5)}$$

which can be transformed to a form similar to (C-1) through (C-3),

$$\rho = \bar{\rho} + 2\sigma c(P). \qquad \text{(C-6)}$$

The form of (C-1) through (C-3) is

$$\rho = m\bar{\rho} + b. \qquad \text{(C-7)}$$

Equating (C-6) and (C-7) and solving for σ gives

$$\sigma = \frac{m - 1}{2\, c(P)}\,\bar{\rho} + \frac{b}{2\, c(P)} \qquad \text{(C-8)}$$

which is an expression for the standard deviation of the absolute humidity in terms of the mean absolute humidity and other knowns. Using the parameters of (C-1) through (C-3) and the appropriate values of c(P) the following three expressions are found:

$$\sigma = 0.0234\bar{\rho} + 2.05 \qquad \text{(C-9)}$$

$$\sigma = 0.0061\bar{\rho} + 2.04 \qquad \text{(C-10)}$$

$$\sigma = -0.0043\bar{\rho} = 2.08. \qquad \text{(C-11)}$$

Bean and Cahoon found (C-1) through (C-3) by least squares fitting data. Using the inverse of the standard errors of their fits as weights, the weighted mean of the coefficients in (C-9) through (C-11) were found. The resulting expression for the standard deviation in terms of the mean absolute humidity for one month (averaged over several years) is

$$\sigma = 0.0094\bar{\rho} + 2.05. \qquad \text{(C-12)}$$

REFERENCES

Bean, B. R., and B. A. Cahoon (1957), A Note on the Climatic Variation of Absolute Humidity, Bull. American Met. Soc., Vol. 38, No. 7, pp. 395-398.

FORM **NTIA-29**
(4-80)

U.S. DEPARTMENT OF COMMERCE
NAT'L. TELECOMMUNICATIONS AND INFORMATION ADMINISTRATION

BIBLIOGRAPHIC DATA SHEET

	1. PUBLICATION NO.	2. Gov't Accession No.	3. Recipient's Accession No.
	NTIA Report 86-192		

4. TITLE AND SUBTITLE

EHF TELECOMMUNICATION SYSTEM ENGINEERING MODEL

5. Publication Date
April 1986

6. Performing Organization Code

7. AUTHOR(S)

Kenneth C. Allen

9. Project/Task/Work Unit No.

8. PERFORMING ORGANIZATION NAME AND ADDRESS

U.S. Dept. of Commerce
NTIA/ITS
325 Broadway
Boulder, CO 80303

10. Contract/Grant No.

11. Sponsoring Organization Name and Address

USAESEIA
Ft. Huachuca, AZ 85613

12. Type of Report and Period Covered

13.

14. SUPPLEMENTARY NOTES

15. ABSTRACT *(A 200-word or less factual summary of most significant information. If document includes a significant bibliography or literature survey, mention it here.)*

An EHF Telecommunication System Engineering Model (ETSEM) has been developed as an aid in the design of line-of-sight (LOS) communication systems from 10 to 100 GHz. ETSEM provides tabulation of path geometry parameters and analyzes ray-path and Fresnel zone clearances to help the engineer design the path. ETSEM also predicts the performance (availability) of both digital and analog systems based on state-of-the-art EHF propagation models and equipment specifications. Attenuation by rain, clear-air absorption, and multipath are modeled. These are expected to essentially determine the statistics of link availability as limited by propagation impairments. Performance may be predicted for any interval of months of the year. A climatological data base for North America and Europe provides parameters for the propagation models. ETSEM has been implemented on a desk-top computer. Weaknesses and limitations of the model are discussed and improvements are suggested.

16. Key Words *(Alphabetical order, separated by semicolons)*

line-of-sight; millimeter wave; telecommunications; propagation; system performance; clear-air absorption; rain attenuation; multipath fading

17. AVAILABILITY STATEMENT	18. Security Class. *(This report)*	20. Number of pages
☒ UNLIMITED.	unclassified	71
☐ FOR OFFICIAL DISTRIBUTION.	19. Security Class. *(This page)*	21. Price

☆ U.S. GOVERNMENT PRINTING OFFICE: 1986—676-002/40,019 REGION NO. 8